



UNIVERSITÄT
HEIDELBERG
ZUKUNFT
SEIT 1386



Parton-pseudo distribution functions from Lattice QCD

Savvas Zafeiropoulos

Universität Heidelberg

15.01.2019

Hirschegg 2019

In collaboration with J. Karpie (College of William & Mary), K. Orginos (College of William & Mary and JLAB), A. Radyushkin (ODU and JLAB) and A. Rothkopf (Stavanger U)

Defining Parton Distribution Functions (PDFs)

- Since the discovery of quarks in DIS experiments at SLAC, PDFs always occupied a key role in HEP
- Large international effort aiming at their measurement
- The target in the DIS experiments can be seen as a stream of partons carrying a fraction x of the longitudinal momentum.
- The momentum distribution functions of partons within the proton are called Parton Distribution Functions (PDFs).
- They represent probability densities to find a parton carrying a fraction x of the nucleon momentum at squared energy scale $Q^2 = -q^2$.
- the uncertainties in PDFs are the dominant, theoretical uncertainties in Higgs couplings and the mass of the W boson.

Defining Parton Distribution Functions (PDFs)

- Since the discovery of quarks in DIS experiments at SLAC, PDFs always occupied a key role in HEP
- Large international effort aiming at their measurement
- The target in the DIS experiments can be seen as a stream of partons carrying a fraction x of the longitudinal momentum.
- The momentum distribution functions of partons within the proton are called Parton Distribution Functions (PDFs).
- They represent probability densities to find a parton carrying a fraction x of the nucleon momentum at squared energy scale $Q^2 = -q^2$.
- the uncertainties in PDFs are the dominant, theoretical uncertainties in Higgs couplings and the mass of the W boson.

Defining Parton Distribution Functions (PDFs)

- Since the discovery of quarks in DIS experiments at SLAC, PDFs always occupied a key role in HEP
- Large international effort aiming at their measurement
- The target in the DIS experiments can be seen as a stream of partons carrying a fraction x of the longitudinal momentum.
- The momentum distribution functions of partons within the proton are called Parton Distribution Functions (PDFs).
- They represent probability densities to find a parton carrying a fraction x of the nucleon momentum at squared energy scale $Q^2 = -q^2$.
- the uncertainties in PDFs are the dominant, theoretical uncertainties in Higgs couplings and the mass of the W boson.

Defining Parton Distribution Functions (PDFs)

- Since the discovery of quarks in DIS experiments at SLAC, PDFs always occupied a key role in HEP
- Large international effort aiming at their measurement
- The target in the DIS experiments can be seen as a stream of partons carrying a fraction x of the longitudinal momentum.
- The momentum distribution functions of partons within the proton are called Parton Distribution Functions (PDFs).
- They represent probability densities to find a parton carrying a fraction x of the nucleon momentum at squared energy scale $Q^2 = -q^2$.
- the uncertainties in PDFs are the dominant, theoretical uncertainties in Higgs couplings and the mass of the W boson.

Defining Parton Distribution Functions (PDFs)

- Since the discovery of quarks in DIS experiments at SLAC, PDFs always occupied a key role in HEP
- Large international effort aiming at their measurement
- The target in the DIS experiments can be seen as a stream of partons carrying a fraction x of the longitudinal momentum.
- The momentum distribution functions of partons within the proton are called Parton Distribution Functions (PDFs).
- They represent probability densities to find a parton carrying a fraction x of the nucleon momentum at squared energy scale $Q^2 = -q^2$.
- the uncertainties in PDFs are the dominant, theoretical uncertainties in Higgs couplings and the mass of the W boson.

Defining Parton Distribution Functions (PDFs)

- Since the discovery of quarks in DIS experiments at SLAC, PDFs always occupied a key role in HEP
- Large international effort aiming at their measurement
- The target in the DIS experiments can be seen as a stream of partons carrying a fraction x of the longitudinal momentum.
- The momentum distribution functions of partons within the proton are called Parton Distribution Functions (PDFs).
- They represent probability densities to find a parton carrying a fraction x of the nucleon momentum at squared energy scale $Q^2 = -q^2$.
- the uncertainties in PDFs are the dominant, theoretical uncertainties in Higgs couplings and the mass of the W boson.

Uncertainties in PDFs

- With the recent impressive development of NNLO higher-order calculations
- that have provided the Higgs gluon fusion cross section at N3LO, with scale uncertainties down to 2%
- PDF uncertainties are now dominant for a number of crucial LHC processes
- Quoting Anastasiou et al *"Finally, the computation of the hadronic cross-section relies crucially on the knowledge of the strong coupling constant and the parton densities. After our calculation, the uncertainty coming from these quantities has become dominant. Further progress in the determination of parton densities must be anticipated in the next few years due to the inclusion of LHC data in the global fits and the impressive advances in NNLO computations, improving the theoretical accuracy of many standard candle processes."*

Phys.Rev.Lett. 114 (2015) 212001

Uncertainties in PDFs

- With the recent impressive development of NNLO higher-order calculations
- that have provided the Higgs gluon fusion cross section at N³LO, with scale uncertainties down to 2%
- PDF uncertainties are now dominant for a number of crucial LHC processes
- Quoting Anastasiou et al *"Finally, the computation of the hadronic cross-section relies crucially on the knowledge of the strong coupling constant and the parton densities. After our calculation, the uncertainty coming from these quantities has become dominant. Further progress in the determination of parton densities must be anticipated in the next few years due to the inclusion of LHC data in the global fits and the impressive advances in NNLO computations, improving the theoretical accuracy of many standard candle processes."*

Phys.Rev.Lett. 114 (2015) 212001

Uncertainties in PDFs

- With the recent impressive development of NNLO higher-order calculations
- that have provided the Higgs gluon fusion cross section at N3LO, with scale uncertainties down to 2%
- PDF uncertainties are now dominant for a number of crucial LHC processes
- Quoting Anastasiou et al *"Finally, the computation of the hadronic cross-section relies crucially on the knowledge of the strong coupling constant and the parton densities. After our calculation, the uncertainty coming from these quantities has become dominant. Further progress in the determination of parton densities must be anticipated in the next few years due to the inclusion of LHC data in the global fits and the impressive advances in NNLO computations, improving the theoretical accuracy of many standard candle processes."*

Phys.Rev.Lett. 114 (2015) 212001

From DIS to PDFs via factorization

- The measurement of PDFs is made possible due to factorization theorems
- Intuitively, factorization theorems (Collins, Soper and Sterman (1989)) tell us that the same universal non-perturbative objects (the PDFs), representing long distance physics, can be combined with many short-distance calculations in QCD to give the cross-sections of various processes.
 - ▶ $\sigma = f \otimes H$, where f are the PDFs, H is the hard perturbative part and \otimes is convolution.
 - ▶ PDFs truly characterize the hadronic target
 - ▶ PDFs are essentially non-perturbative

From DIS to PDFs via factorization

- The measurement of PDFs is made possible due to factorization theorems
- Intuitively, factorization theorems (Collins, Soper and Sterman (1989)) tell us that the same universal non-perturbative objects (the PDFs), representing long distance physics, can be combined with many short-distance calculations in QCD to give the cross-sections of various processes.
 - ▶ $\sigma = f \otimes H$, where f are the PDFs, H is the hard perturbative part and \otimes is convolution.
 - ▶ PDFs truly characterize the hadronic target
 - ▶ PDFs are essentially non-perturbative

From DIS to PDFs via factorization

- The measurement of PDFs is made possible due to factorization theorems
- Intuitively, factorization theorems (Collins, Soper and Sterman (1989)) tell us that the same universal non-perturbative objects (the PDFs), representing long distance physics, can be combined with many short-distance calculations in QCD to give the cross-sections of various processes.
 - ▶ $\sigma = f \otimes H$, where f are the PDFs, H is the hard perturbative part and \otimes is convolution.
 - ▶ PDFs truly characterize the hadronic target
 - ▶ PDFs are essentially non-perturbative

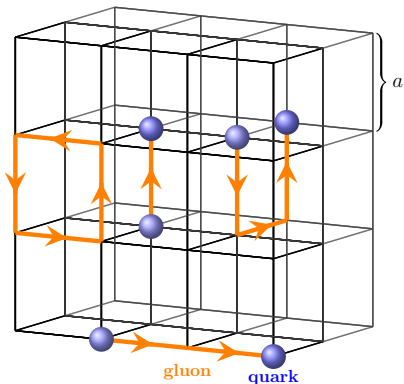
From DIS to PDFs via factorization

- The measurement of PDFs is made possible due to factorization theorems
- Intuitively, factorization theorems (Collins, Soper and Sterman (1989)) tell us that the same universal non-perturbative objects (the PDFs), representing long distance physics, can be combined with many short-distance calculations in QCD to give the cross-sections of various processes.
 - ▶ $\sigma = f \otimes H$, where f are the PDFs, H is the hard perturbative part and \otimes is convolution.
 - ▶ PDFs truly characterize the hadronic target
 - ▶ PDFs are essentially non-perturbative

From DIS to PDFs via factorization

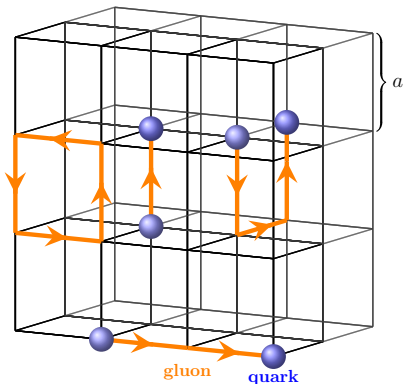
- The measurement of PDFs is made possible due to factorization theorems
- Intuitively, factorization theorems (Collins, Soper and Sterman (1989)) tell us that the same universal non-perturbative objects (the PDFs), representing long distance physics, can be combined with many short-distance calculations in QCD to give the cross-sections of various processes.
 - ▶ $\sigma = f \otimes H$, where f are the PDFs, H is the hard perturbative part and \otimes is convolution.
 - ▶ PDFs truly characterize the hadronic target
 - ▶ PDFs are essentially non-perturbative

Lattice?



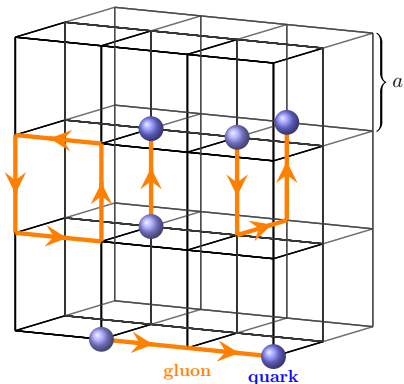
- The natural ab-initio method to study QCD non-perturbatively is on the lattice. But ...
- PDFs are defined as an expectation value of a bilocal operator evaluated along a light-like line.
- Clearly, we can not evaluate this on a Euclidean set-up.

Lattice?



- The natural ab-initio method to study QCD non-perturbatively is on the lattice. But ...
- PDFs are defined as an expectation value of a bilocal operator evaluated along a light-like line.
- Clearly, we can not evaluate this on a Euclidean set-up.

Lattice?



- The natural ab-initio method to study QCD non-perturbatively is on the lattice. But ...
- PDFs are defined as an expectation value of a bilocal operator evaluated along a light-like line.
- Clearly, we can not evaluate this on a Euclidean set-up.

Lattice traditionally

- Mellin moments of PDFs via matrix elements (ME) of twist-2 operators.
- Light cone PDF

$$f^{(0)}(\xi) = \frac{1}{4\pi} \int_{-\infty}^{\infty} d\omega^- e^{-i\xi P^+ \omega^-} \langle P | T \bar{\psi}(0, \omega^-, 0_{\perp}) W(\omega^-, 0) \gamma^+ \frac{\lambda^a}{2} \psi(0) | P \rangle_C$$

$$\text{where } W(\omega^-, 0) = \mathcal{P} \exp \left[-ig_0 \int_0^{\omega^-} dy^- A_{\alpha}^+(0, y^-, 0_{\perp}) T_{\alpha} \right]$$

- Moments are defined as

$$a_0^{(n)} = \int_0^1 d\xi \xi^{n-1} \left[f^{(0)}(\xi) + (-1)^n \bar{f}^{(0)}(\xi) \right] = \int_{-1}^1 d\xi \xi^{n-1} f(\xi)$$

related to local ME $\langle P | \mathcal{O}_0^{\mu_1, \dots, \mu_n} | P \rangle = 2a_0^{(n)} (P^{\mu_1} \dots P^{\mu_n} - \text{traces})$ where

$$\mathcal{O}_0^{\mu_1, \dots, \mu_n} = i^{n-1} \bar{\psi}(0) \gamma^{\{\mu_1} D^{\mu_2} \dots D^{\mu_n\}} \frac{\lambda^a}{2} \psi(0) - \text{traces}$$

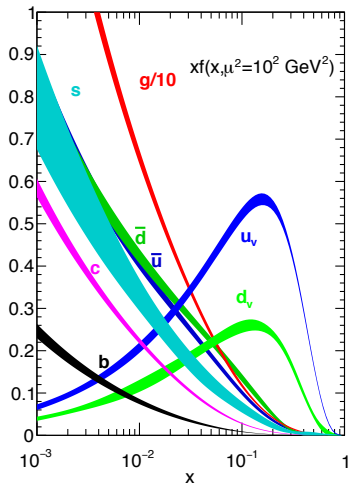
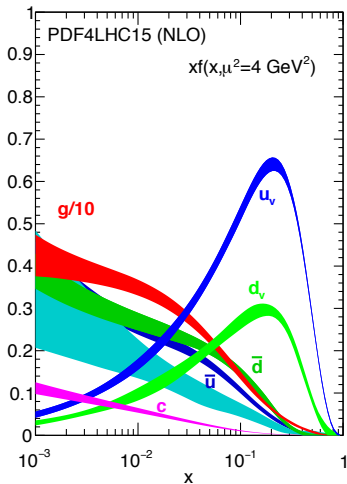
Lattice traditionally

- Would not be an issue if every moment were accessible because a probability distribution is completely determined once all its moments are known.
- These studies are limited to the first few (three) moments due to
 - ▶ Bad signal to noise ratio
 - ▶ Power-divergent mixing on the lattice (discretized space-time does not possess the full rotational symmetry of the continuum).

Global PDF fits

- Realize a QCD analysis of hard-scattering measurements employing a variety of hadronic observables
- Parton densities parametrized @ an initial energy scale evolved up to the scale of data via DGLAP eqs.
- Build theoretical predictions for the observables.
- Best fit parameters determined by the minimization of an appropriate figure of merit (eg. χ^2).
- Many free parameters
- Advanced techniques (eg. use of neural networks).

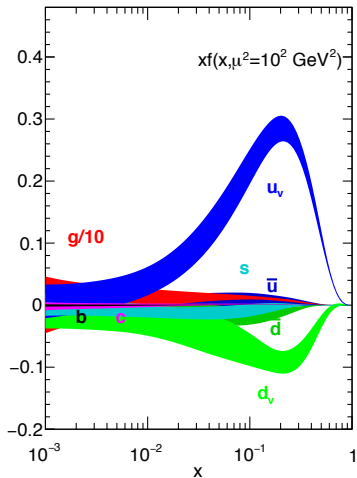
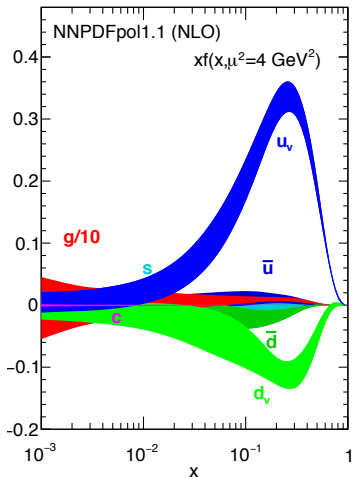
Determination of PDFs from Experiment



Global fits to experimental data [Parton distributions and lattice QCD calculations: a community white paper arXiv:1711.07916](#)

1711.07916

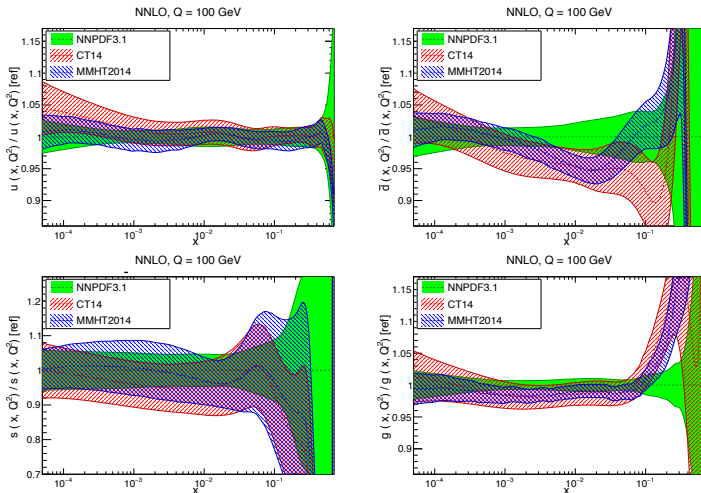
Determination of PDFs from Experiment



Global fits to experimental data [Parton distributions and lattice QCD calculations: a community white paper arXiv:1711.07916](#)

1711.07916

Determination of PDFs from Experiment



Global fits to experimental data [Parton distributions and lattice QCD calculations: a community white paper arXiv:1711.07916](#)

1711.07916

Light-like is a NO-GO

Hadronic Tensor Methods

- “Light-like” separated Hadronic Tensor K. F. Liu et al Phys.Rev.Lett. 72 (1994), A. J. Chambers et al Phys.Rev.Lett. 118 (2017)

Ioffe Time Pseudo Distribution Methods

- quasi-PDFs (X. Ji Phys.Rev.Lett. 110, (2013))
- pseudo-PDFs (A. Radyushkin Phys.Lett. B767 (2017))

Similarly to a global QCD analysis of high energy scattering data, PDFs can also be extracted from analyzing data generated by lattice-QCD calculation of good lattice cross-sections Y.-Q. Ma and J.-W. Qiu Phys. Rev. Lett. 120 (2018)

Formalism

Computing PDFs in LQCD we start from the equal time hadronic matrix element with the quark and anti-quark fields separated by a finite distance. For non-singlet parton densities the matrix element

$$\mathcal{M}^\alpha(z, p) \equiv \langle p | \bar{\psi}(0) \gamma^\alpha \hat{E}(0, z; A) \tau_3 \psi(z) | p \rangle$$

where $\hat{E}(0, z; A)$ is the $0 \rightarrow z$ straight-line gauge link in the fundamental representation, τ_3 is the flavor Pauli matrix, and γ^α is a gamma matrix. We can decompose the matrix element due to Lorentz invariance as

$$\mathcal{M}^\alpha(z, p) = 2p^\alpha \mathcal{M}_p(-(zp), -z^2) + z^\alpha \mathcal{M}_z(-(zp), -z^2)$$

Formalism

- From the $\mathcal{M}_p(-(zp), -z^2)$ part the twist-2 contribution to PDFs can be obtained in the limit $z^2 \rightarrow 0$.
- By taking $z = (0, 0, 0, z_3)$, α in the temporal direction i.e. $\alpha = 0$, and the hadron momentum $p = (p^0, 0, 0, p)$ the z^α -part drops out.
- The Lorentz invariant quantity $\nu = -(zp)$, is the "Ioffe time" (B. L. Ioffe, Phys. Lett. 30B, 123 (1969)) and

$$\langle p | \bar{\psi}(0) \gamma^0 \hat{E}(0, z; A) \tau_3 \psi(z) | p \rangle = 2p^0 \mathcal{M}_p(\nu, z_3^2)$$

Formalism

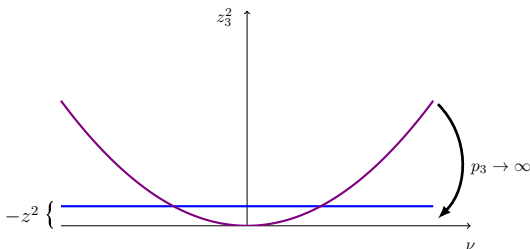
- The quasi-PDF $Q(x, p^2)$ is related to $\mathcal{M}_p(\nu, z_3^2)$ by

$$Q(x, p^2) = \frac{1}{2\pi} \int_{-\infty}^{\infty} d\nu e^{-ix\nu} \mathcal{M}_p(\nu, [\nu/p]^2)$$

Quasi PDF mixes invariant scales until p_z is effectively large enough

- While the pseudo-PDF has fixed invariant scale dependence

$$P(x, z_0^2) = \frac{1}{2\pi} \int_{-\infty}^{\infty} d\nu e^{-ix\nu} \mathcal{M}_p(\nu, z_0^2)$$



Lattice QCD requirements

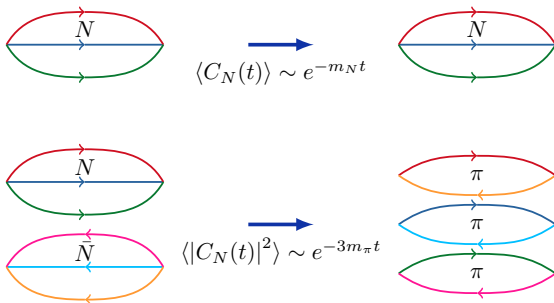
- Largest momentum on the lattice $aP_{max} = \pi/2 \propto \mathcal{O}(1)$
- $a = 0.1\text{fm} \rightarrow P_{max} = 10\Lambda$ where $\Lambda = 300 \text{ MeV}$
- $a = 0.05\text{fm} \rightarrow P_{max} = 20\Lambda$

Large momentum is required to suppress high twist effects (quasi-PDFs) and to provide a wide coverage of the loffe time ν

$P_{max} = 3 \text{ GeV}$ easily achievable with moderate values of the lattice spacing but still demanding due to statistical noise

$P_{max} = 6 \text{ GeV}$ exponentially harder requiring very fine values of the lattice spacing

Signal to Noise



Statistical accuracy drops exponentially with increasing momentum P

$$\text{StN}(O) = \frac{\langle O \rangle}{\sqrt{\text{var}(O)}} \propto e^{-[E_N(P) - 3/2m_\pi]t}$$

G. Parisi (1984) P. Lepage (1989)

Formalism

loffe time PDFs $\mathcal{M}(\nu, z_3^2)$ defined at a scale $\mu^2 = 4e^{-2\gamma_E}/z_3^2$ (at leading log level) are the Fourier transform of regular PDFs $f(x, \mu^2)$. (I.I. Balitsky and V.M. Braun, Nucl.

Phys. B311, 541 (1988), V. Braun, et. al Phys. Rev. D 51, 6036 (1995))

$$\mathcal{M}(\nu, z_3^2) = \int_{-1}^1 dx f(x, 1/z_3^2) e^{ix\nu}$$

Scale dependence of the loffe time PDF derived from the DGLAP evolution of the regular PDFs.

loffe time PDFs evolution equation

$$\frac{d}{d \ln z_3^2} \mathcal{M}(\nu, z_3^2) = -\frac{\alpha_s}{2\pi} C_F \int_0^1 du B(u) \mathcal{M}(u\nu, z_3^2)$$

with $B(u) = \left[\frac{1+u^2}{1-u} \right]_+$, $C_F = 4/3$, and $B(u)$ is the LO evolution kernel for the non-singlet quark PDF (V. Braun, et. al Phys. Rev. D 51, 6036 (1995))

Obtaining the Ioffe time PDF

$$z_3 \rightarrow 0 \Rightarrow \mathcal{M}_p(\nu, z_3^2) = \mathcal{M}(\nu, z_3^2) + \mathcal{O}(z_3^2)$$

But.... large $\mathcal{O}(z_3^2)$ corrections prohibit the extraction.

Conservation of the vector current implies $\mathcal{M}_p(0, z_3^2) = 1 + \mathcal{O}(z_3^2)$, but in a ratio z_3^2 corrections (related to the transverse structure of the hadron) might cancel (A. Radyushkin Phys.Lett. B767 (2017))

$$\mathfrak{M}(\nu, z_3^2) \equiv \frac{\mathcal{M}_p(\nu, z_3^2)}{\mathcal{M}_p(0, z_3^2)}$$

- Much smaller $\mathcal{O}(z_3^2)$ corrections and therefore this ratio could be used to extract the Ioffe time PDFs
- All UV singularities are exactly cancelled and when computed in lattice QCD it can be extrapolated to the continuum limit at fixed ν and z^2 .

Numerical implementation

First case study in an unphysical setup

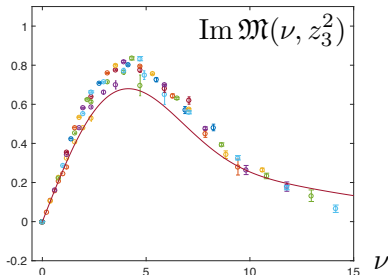
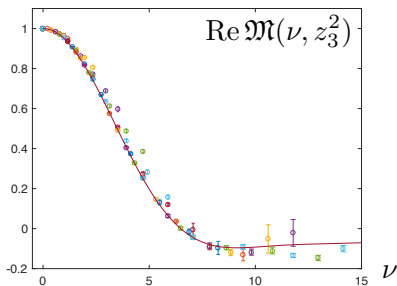
- Quenched approximation
- $32^3 \times 64$ lattices with $a = 0.093\text{fm}$.
- $m_\pi = 601\text{MeV}$ and $m_N = 1411\text{MeV}$

Now employing dynamical ensembles (preliminary)

$a(\text{fm})$	$M_\pi(\text{MeV})$	β	$L^3 \times T$
0.127(2)	440	6.1	$24^3 \times 64$
0.127(2)	440	6.1	$32^3 \times 96$
0.094(1)	400	6.3	$32^3 \times 64$
0.094(1)	280	6.3	$32^3 \times 64$
0.094(1)	172	6.3	$64^3 \times 128$

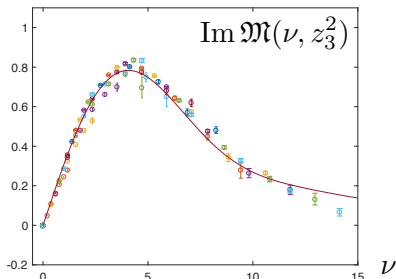
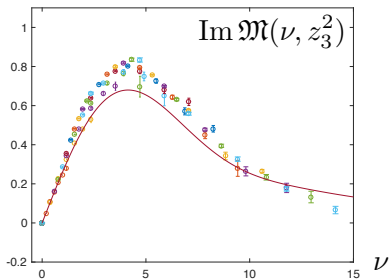
Table: Parameters for the lattices generated by the JLab/W&M collaboration using 2+1 flavors of clover Wilson fermions and a tree-level tadpole-improved Symanzik gauge action. The lattice spacings, a , are estimated using the Wilson flow scale w_0 . Stout smearing implemented in the fermion action makes the tadpole corrected tree-level clover coefficient c_{SW} used, to be very close to the value determined non-pertubatively with the Schrödinger functional method

Results for the Re and Im parts of $\mathfrak{M}(\nu, z_3^2)$



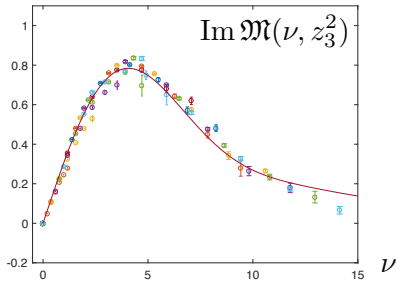
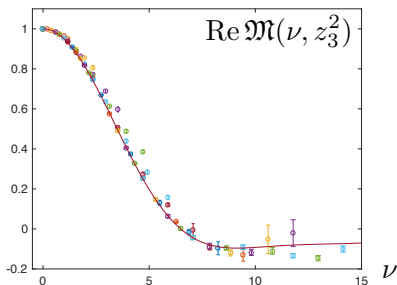
- Curves represent Re and Im Fourier transforms of $q_\nu(x) = \frac{315}{32} \sqrt{x}(1-x)^3$.
- Considering CP even and odd combinations
 - ▶ even: $q_-(x) = f(x) + f(-x) = q(x) - \bar{q}(x) = q_\nu(x)$
 - ▶ odd: $q_+(x) = f(x) - f(-x) = q(x) + \bar{q}(x) = q_\nu(x) + 2\bar{q}(x)$

Results for the Im part of $\mathfrak{M}(\nu, z_3^2)$



- Curves represent the Im Fourier transforms of $q_v(x) = q(x) - \bar{q}(x)$ and $q_+(x) = q(x) + \bar{q}(x) = q_v(x) + 2\bar{q}(x)$ respectively.
- The agreement with the data is strongly improved if we use a non-vanishing antiquark contribution, namely $\bar{q}(x) = \bar{u}(x) + \bar{d}(x) = 0.07[20x(1-x)^3]$.

Results for the Re and Im parts of $\mathfrak{M}(\nu, z_3^2)$



- Data as function of the loffe time. A residual z_3 -dependence can be seen.
- This is more visible when, for a particular ν we have several data points corresponding to different values of z_3 .
- Different values of z_3^2 for the same ν correspond to the loffe time distribution at different scales.

Residual z_3 -dependence

- Is the residual scatter in the data points consistent with evolution? By solving the evolution equation at LO, the Ioffe time PDF at z'_3 is related to the one at z_3 by

$$\mathfrak{M}(\nu, z'_3{}^2) = \mathfrak{M}(\nu, z_3^2) - \frac{2}{3} \frac{\alpha_s}{\pi} \ln(z'_3{}^2/z_3^2) \int_0^1 du B(u) \mathfrak{M}(u\nu, z_3^2)$$

- Only applicable at small z_3
- Check its effect using data at values of $z_3 \leq 4a$ corresponding to energy scales larger than 500 MeV.
- We fix the point z'_3 at the value $z_0 = 2a$ corresponding, at leading logarithm level, to the $\overline{\text{MS}}$ -scheme scale $\mu_0 = 1$ GeV and evolve the rest of the points to that scale.

Residual z_3 -dependence

- Is the residual scatter in the data points consistent with evolution? By solving the evolution equation at LO, the Ioffe time PDF at z'_3 is related to the one at z_3 by

$$\mathfrak{M}(\nu, z'^2_3) = \mathfrak{M}(\nu, z^2_3) - \frac{2}{3} \frac{\alpha_s}{\pi} \ln(z'^2_3 / z^2_3) \int_0^1 du B(u) \mathfrak{M}(u\nu, z^2_3)$$

- Only applicable at small z_3
- Check its effect using data at values of $z_3 \leq 4a$ corresponding to energy scales larger than 500 MeV.
- We fix the point z'_3 at the value $z_0 = 2a$ corresponding, at leading logarithm level, to the $\overline{\text{MS}}$ -scheme scale $\mu_0 = 1$ GeV and evolve the rest of the points to that scale.

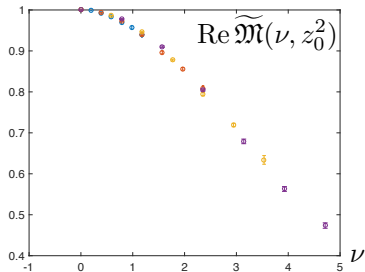
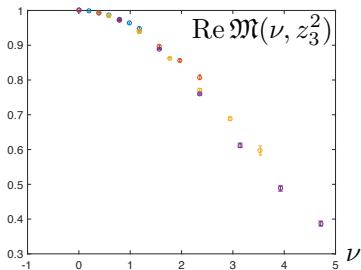
Residual z_3 -dependence

- Is the residual scatter in the data points consistent with evolution? By solving the evolution equation at LO, the Ioffe time PDF at z'_3 is related to the one at z_3 by

$$\mathfrak{M}(\nu, z_3'^2) = \mathfrak{M}(\nu, z_3^2) - \frac{2}{3} \frac{\alpha_s}{\pi} \ln(z_3'^2/z_3^2) \int_0^1 du B(u) \mathfrak{M}(u\nu, z_3^2)$$

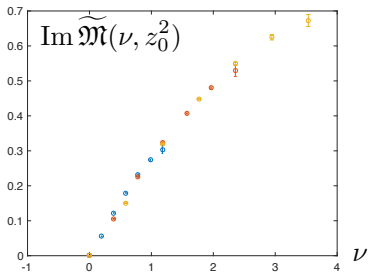
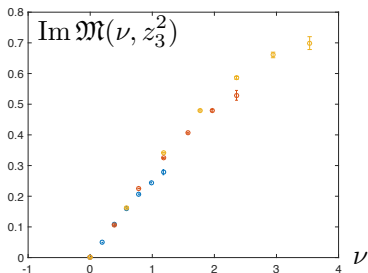
- Only applicable at small z_3
- Check its effect using data at values of $z_3 \leq 4a$ corresponding to energy scales larger than 500 MeV.
- We fix the point z_3' at the value $z_0 = 2a$ corresponding, at leading logarithm level, to the $\overline{\text{MS}}$ -scheme scale $\mu_0 = 1$ GeV and evolve the rest of the points to that scale.

Before and after evolution



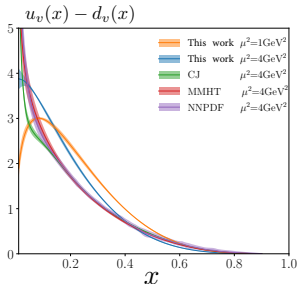
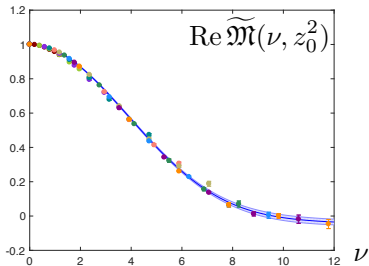
The ratio $\mathfrak{M}(\nu, z_3^2)$ for $z_3/a = 1, 2, 3, \text{ and } 4$. **LHS:** Data before evolution. **RHS:** Data after evolution. The reduction in scatter indicates that evolution collapses all data to the same universal curve.

Before and after evolution



The ratio $\mathfrak{M}(\nu, z_3^2)$ for $z_3/a = 1, 2, 3,$ and 4 . **LHS:** Data before evolution. **RHS:** Data after evolution. The reduction in scatter indicates that evolution collapses all data to the same universal curve.

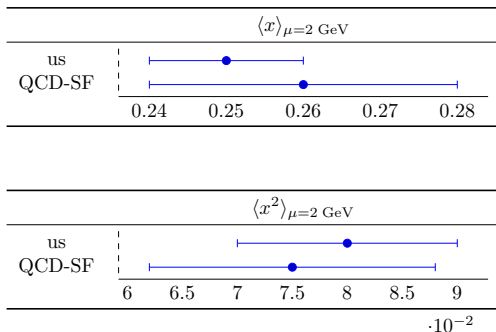
Comparison to global fits



LHS: Data points for $\text{Re } \widetilde{\mathfrak{M}}(\nu, z_3^2)$ with $z_3 \leq 10a$ evolved to $z_3 = 2a$. By fitting these evolved points with a cosine FT of $q_v(x) = N(a, b)x^a(1-x)^b$ we obtain $a = 0.36(6)$ and $b = 3.95(22)$ (statistical errors). RHS: Curve for $u_v(x) - d_v(x)$ built from the evolved data shown in the left panel and treated as corresponding to the $\mu^2 = 1 \text{ GeV}^2$ scale; then evolved to the reference point $\mu^2 = 4 \text{ GeV}^2$ of the global fits.

Sanity checks vs other lattice results

- One can try to extract the lowest PDF moments from our data and compare with the lattice literature [QCD-SF collaboration Phys.Rev. D53 \(1996\) 2317-2325](#)
- With the Wilson coefficients computed we can now obtain the \overline{MS} moments up to $\mathcal{O}(\alpha_s^2, z^2)$ directly from the reduced function $\mathfrak{M}(\nu, z^2)$ as
- $$a_{n+1}(\mu) = (-i)^n \frac{1}{c_n(z^2\mu^2)} \left. \frac{\partial^n \mathfrak{M}(\nu, z^2)}{\partial \nu^n} \right|_{\nu=0} + \mathcal{O}(z^2, \alpha_s^2)$$



Reconstruction

- Parton distribution functions (PDF) or distribution amplitudes (DA) may be defined in lattice QCD by inverting the quasi-Fourier transform of a certain class of hadronic position space matrix elements.
- One particular example are the Ioffe-time PDFs \mathfrak{M}_R , which are related to the physical PDF via the integral relation

$$\mathfrak{M}_R(\nu, \mu^2) \equiv \int_0^1 dx \cos(\nu x) q_v(x, \mu^2).$$

- Here it is assumed that the lattice computed matrix element is converted to the \overline{MS} Ioffe-time PDF at a scale μ^2 , using a perturbative kernel as discussed in [Radyushkin \(Phys.Rev. D98 \(2018\) no.1, 014019\)](#), [Zhang et al Phys.Rev. D97 \(2018\) no.7, 074508](#)
- The task at hand is then to reconstruct the PDF $q_v(x, \mu^2)$ given a limited set of simulated data for $\mathfrak{M}_R(\nu, \mu^2)$.

Reconstruction

- Parton distribution functions (PDF) or distribution amplitudes (DA) may be defined in lattice QCD by inverting the quasi-Fourier transform of a certain class of hadronic position space matrix elements.
- One particular example are the Ioffe-time PDFs \mathfrak{M}_R , which are related to the physical PDF via the integral relation

$$\mathfrak{M}_R(\nu, \mu^2) \equiv \int_0^1 dx \cos(\nu x) q_v(x, \mu^2).$$

- Here it is assumed that the lattice computed matrix element is converted to the \overline{MS} Ioffe-time PDF at a scale μ^2 , using a perturbative kernel as discussed in [Radyushkin \(Phys.Rev. D98 \(2018\) no.1, 014019\)](#), [Zhang et al Phys.Rev. D97 \(2018\) no.7, 074508](#)
- The task at hand is then to reconstruct the PDF $q_v(x, \mu^2)$ given a limited set of simulated data for $\mathfrak{M}_R(\nu, \mu^2)$.

Reconstruction

- Parton distribution functions (PDF) or distribution amplitudes (DA) may be defined in lattice QCD by inverting the quasi-Fourier transform of a certain class of hadronic position space matrix elements.
- One particular example are the Ioffe-time PDFs \mathfrak{M}_R , which are related to the physical PDF via the integral relation

$$\mathfrak{M}_R(\nu, \mu^2) \equiv \int_0^1 dx \cos(\nu x) q_v(x, \mu^2).$$

- Here it is assumed that the lattice computed matrix element is converted to the \overline{MS} Ioffe-time PDF at a scale μ^2 , using a perturbative kernel as discussed in [Radyushkin \(Phys.Rev. D98 \(2018\) no.1, 014019\)](#), [Zhang et al Phys.Rev. D97 \(2018\) no.7, 074508](#)
- The task at hand is then to reconstruct the PDF $q_v(x, \mu^2)$ given a limited set of simulated data for $\mathfrak{M}_R(\nu, \mu^2)$.

Reconstruction

- Parton distribution functions (PDF) or distribution amplitudes (DA) may be defined in lattice QCD by inverting the quasi-Fourier transform of a certain class of hadronic position space matrix elements.
- One particular example are the Ioffe-time PDFs \mathfrak{M}_R , which are related to the physical PDF via the integral relation

$$\mathfrak{M}_R(\nu, \mu^2) \equiv \int_0^1 dx \cos(\nu x) q_v(x, \mu^2).$$

- Here it is assumed that the lattice computed matrix element is converted to the \overline{MS} Ioffe-time PDF at a scale μ^2 , using a perturbative kernel as discussed in [Radyushkin \(Phys.Rev. D98 \(2018\) no.1, 014019\)](#), [Zhang et al Phys.Rev. D97 \(2018\) no.7, 074508](#)
- The task at hand is then to reconstruct the PDF $q_v(x, \mu^2)$ given a limited set of simulated data for $\mathfrak{M}_R(\nu, \mu^2)$.

Reconstruction

- There exist two challenges to this endeavor, the first being that the integral in question does *not extend over the full Brillouin zone*, the second that in practice only a *small number of points along ν* can be computed.
- As we will discuss in more detail below, taken together these issues render the extraction highly ill-posed and we explore different regularization strategies on how to nevertheless reliably estimate the PDF from the data at hand.
- Phenomenological investigations of PDFs have shown that their functional form may be reasonably well approximated by the following simple Ansatz

$$p(x) = \frac{\Gamma(a+b+2)}{\Gamma(a+1)\Gamma(b+1)} x^a (1-x)^b .$$

Reconstruction

- There exist two challenges to this endeavor, the first being that the integral in question does *not extend over the full Brillouin zone*, the second that in practice only a *small number of points along ν* can be computed.
- As we will discuss in more detail below, taken together these issues render the extraction highly ill-posed and we explore different regularization strategies on how to nevertheless reliably estimate the PDF from the data at hand.
- Phenomenological investigations of PDFs have shown that their functional form may be reasonably well approximated by the following simple Ansatz

$$p(x) = \frac{\Gamma(a+b+2)}{\Gamma(a+1)\Gamma(b+1)} x^a (1-x)^b.$$

Reconstruction

- There exist two challenges to this endeavor, the first being that the integral in question does *not extend over the full Brillouin zone*, the second that in practice only a *small number of points along ν* can be computed.
- As we will discuss in more detail below, taken together these issues render the extraction highly ill-posed and we explore different regularization strategies on how to nevertheless reliably estimate the PDF from the data at hand.
- Phenomenological investigations of PDFs have shown that their functional form may be reasonably well approximated by the following simple Ansatz

$$p(x) = \frac{\Gamma(a + b + 2)}{\Gamma(a + 1)\Gamma(b + 1)} x^a (1 - x)^b .$$

Naive Reconstruction

- Discretize the integral, employing the trapezoid integration rule

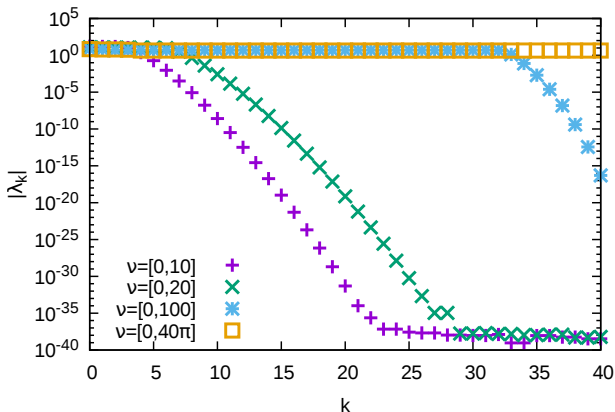
- $\Delta x = \frac{1}{N_x}$, $x_k = k\Delta x = \frac{k}{N_x}$

$$\mathfrak{M}_R(\nu) = \frac{1}{2} \cos(\nu x_0) q_v(x_0) + \sum_{k=1}^{N_x-1} \delta x \cos(\nu x_k) q_v(x_k) + \frac{1}{2} \cos(\nu x_{N_x}) q_v(x_{N_x})$$

We can determine the unknown values of the function $q_v(x_k)$ by solving a simple linear system of equations.

- Defining $\mathfrak{m}_k = \mathfrak{M}_R(\nu_k)$ where ν_k are the values of the loffe time for which data is available and \mathfrak{q} be the vector with components the unknown values of $q_v(x_k)$ i.e. $\mathfrak{q}_k = q_v(x_k)$. Our problem is cast in a matrix equation $\mathfrak{m} = \mathfrak{C} \cdot \mathfrak{q}$,
- The conditioning of the problem is easily elucidated by considering the eigenvalues of the matrix \mathfrak{C} .

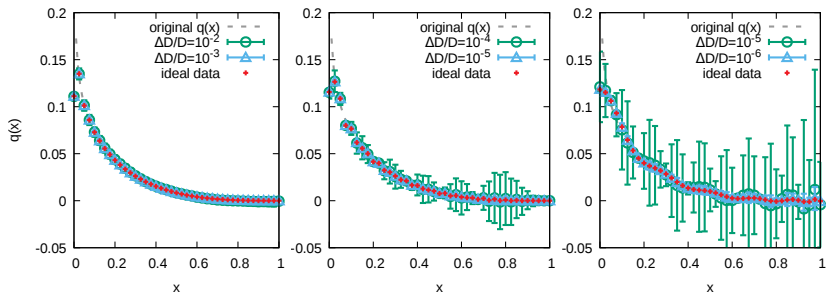
Naive Reconstruction



Eigenvalues λ_k of the kernel matrix for various discretization intervals.

Only for the case corresponding to a genuine discrete Fourier transform $\nu = [0, 40\pi]$ all eigenvalues remain of order unity. The realistic case of $\nu = [0, 20]$ already shows a significant degradation of the spectrum.

Naive Reconstruction



Results for the direct inversion for different discretization intervals (left $\nu = [0, 40\pi]$, center $\nu = [0, 100]$, right $\nu = [0, 20]$). Note the different size of the relative errors needed, to obtain a well behaved result (left $\Delta \mathfrak{M}_R / \mathfrak{M}_R = 10^{-2}$, center $\Delta \mathfrak{M}_R / \mathfrak{M}_R = 10^{-5}$, right $\Delta \mathfrak{M}_R / \mathfrak{M}_R = 10^{-6}$).

Advanced PDF Reconstructions

- A versatile approach is Bayesian inference Y. Burnier and A. Rothkopf Phys.Rev.Lett. 111 (2013)
- It acknowledges the fact that the inverse problem is ill-defined and a unique answer may only be provided, once further information about the system has been made available.
- Formulated in terms of probabilities, one finds in the form of Bayes theorem that

$$P[q|\mathfrak{M}, I] = \frac{P[\mathfrak{M}|q, I]P[q|I]}{P[\mathfrak{M}|I]}.$$

It states that the so called **posterior probability** $P[q|\mathfrak{M}, I]$ for a test function q to be the correct x -space PDF, given our simulated loffe-time PDF \mathfrak{M} and additional prior information may be expressed in terms of three quantities.

Advanced PDF Reconstructions

- A versatile approach is Bayesian inference Y. Burnier and A. Rothkopf Phys.Rev.Lett. 111 (2013)
- It acknowledges the fact that the inverse problem is ill-defined and a unique answer may only be provided, once further information about the system has been made available.
- Formulated in terms of probabilities, one finds in the form of Bayes theorem that

$$P[q|\mathfrak{M}, I] = \frac{P[\mathfrak{M}|q, I]P[q|I]}{P[\mathfrak{M}|I]}.$$

It states that the so called **posterior probability** $P[q|\mathfrak{M}, I]$ for a test function q to be the correct x -space PDF, given our simulated loffe-time PDF \mathfrak{M} and additional prior information may be expressed in terms of three quantities.

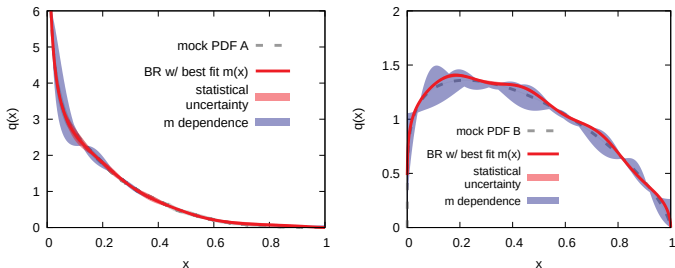
Advanced PDF Reconstructions

- A versatile approach is Bayesian inference Y. Burnier and A. Rothkopf Phys.Rev.Lett. 111 (2013)
- It acknowledges the fact that the inverse problem is ill-defined and a unique answer may only be provided, once further information about the system has been made available.
- Formulated in terms of probabilities, one finds in the form of Bayes theorem that

$$P[q|\mathfrak{M}, I] = \frac{P[\mathfrak{M}|q, I]P[q|I]}{P[\mathfrak{M}|I]}.$$

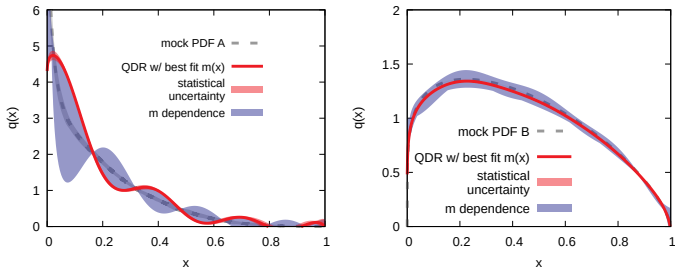
It states that the so called **posterior probability** $P[q|\mathfrak{M}, I]$ for a test function q to be the correct x -space PDF, given our simulated loffe-time PDF \mathfrak{M} and additional prior information may be expressed in terms of three quantities.

Bayesian Reconstruction



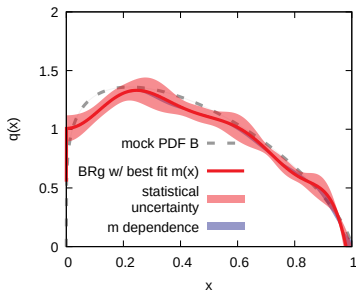
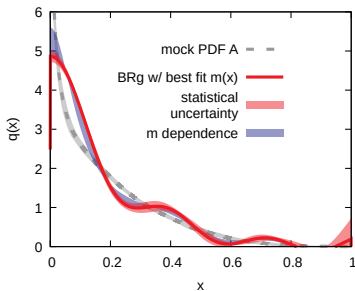
x -space PDF's reconstructed using the BR method from $N_\nu = 10$ loffe-time data points on the interval $\nu = [0, 20]$ The plots in the left column denote the results for mock data based on a phenomenological PDF (NNPDF31_nnlo_as_0118), while the right column arises from a scenario where $q(0)$ is finite.

Bayesian Reconstruction



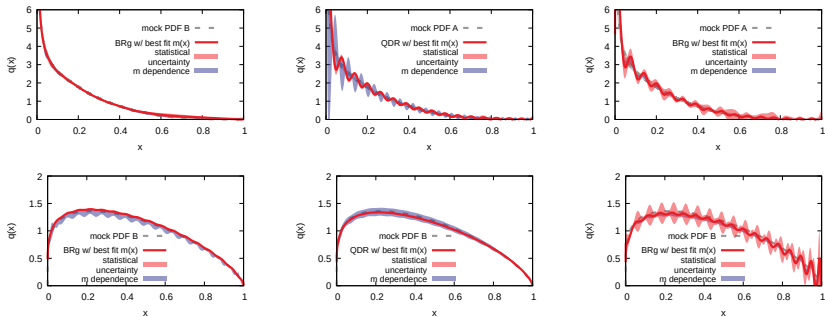
x -space PDF's reconstructed using a quadratic prior Bayesian (QDR) method from $N_\nu = 10$ loffe-time data points on the interval $\nu = [0, 20]$. The plots in the left column denote the results for mock data based on a phenomenological PDF (NNPDF31_nn1o_as_0118), while the right column arises from a scenario where $q(0)$ is finite.

Bayesian Reconstruction



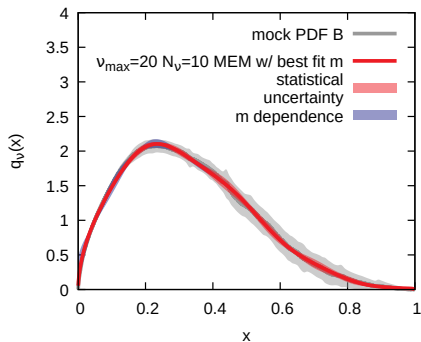
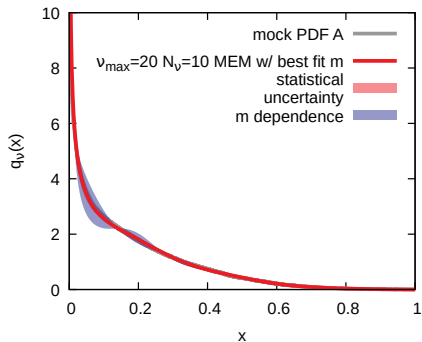
x -space PDF's reconstructed using the generalized Bayesian reconstruction (BRg) method from $N_\nu = 10$ loffe-time data points on the interval $\nu = [0, 20]$. The plots in the left column denote the results for mock data based on a phenomenological PDF (NNPDF31_nn1o_as_0118), while the right column arises from a scenario where $q(0)$ is finite.

Bayesian Reconstruction



x -space PDF's reconstructed in a best case scenario ($\nu = [0, 100]$, $N_\nu = 100$) using (left) the BR method (center) the quadratic prior and (right) the generalized BR method. The input data again is the one from a (top) $N_\nu = 100$ discretized loffe-time realistic PDF, while the bottom row arises from a scenario where $q(0)$ is finite.

Maximum Entropy Method Reconstruction



Backus-Gilbert Reconstruction

- The Backus-Gilbert (BG) method instead of imposing a smoothing condition on the resulting PDF $q(x)$ it imposes a minimization condition on the variance of the resulting function. G. Backus and F. Gilbert. *Geophysical Journal of the Royal*

Astronomical Society, 16:169205, (1968)

- Let us define a rescaled kernel and rescaled PDF $h(x)$

$$K_j(x) \equiv \cos(\nu_j x) p(x) \quad \text{and} \quad h(x) \equiv \frac{q_v(x)}{p(x)}$$

- where $p(x)$ corresponds to an appropriately chosen function that makes the problem easier to solve.
- We wish to incorporate into $p(x)$ most of the non-trivial structure of $q(x)$ apriorily, such that $h(x)$ is a slowly varying function of x and contains only the deviation of $q(x)$ from $p(x)$.

Backus-Gilbert Reconstruction

- Starting from the preconditioned expression with a rescaled PDF $h(x)$ that is only a slowly varying function of x our inverse problem becomes

$$d_j \equiv \mathfrak{M}_R(\nu_j) = \int_0^1 dx K_j(x) h(x).$$

- BG introduces a function $\Delta(x - \bar{x}) = \sum_j q_j(\bar{x}) K_j(x)$, where $q_j(\bar{x})$ are unknown functions to be determined.
- It then estimates the unknown function as a linear combination of the data

$$\hat{h}(\bar{x}) = \sum_j q_j(\bar{x}) d_j, \text{ or } \hat{q}_v(\bar{x}) = \sum_j q_j(\bar{x}) d_j p(\bar{x})$$

- If $\Delta(x - \bar{x})$ were to be a δ -function then $\hat{h}(\bar{x}) = h(\bar{x})$. If $\Delta(x - \bar{x})$ approximates a δ -function with a width σ , then the smaller σ is the better the approximation of $\hat{h}(x)$ to $h(x)$.

Backus-Gilbert Reconstruction

- In other words if $\hat{h}_\sigma(x)$ is the approximation resulting from $\Delta(x)$ with a width σ then $\lim_{\sigma \rightarrow 0} \hat{h}_\sigma(x) = h(x)$.
- With this in mind BG minimizes the width σ given by

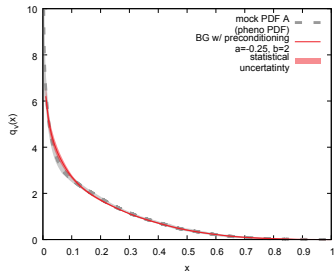
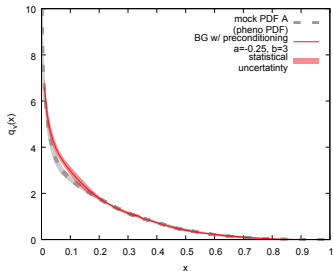
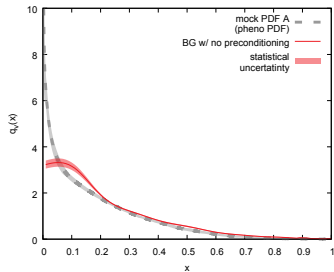
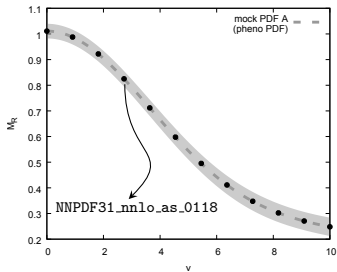
$$\sigma = \int_0^1 dx (x - \bar{x})^2 \Delta(x - \bar{x})^2.$$

- Furthermore, if $\Delta(x)$ approximates a δ -function then one has to impose the constraint $\int_0^1 dx \Delta(x - \bar{x}) = 1$. Using a Lagrange multiplier λ one can minimize the width and impose the constraint by minimizing

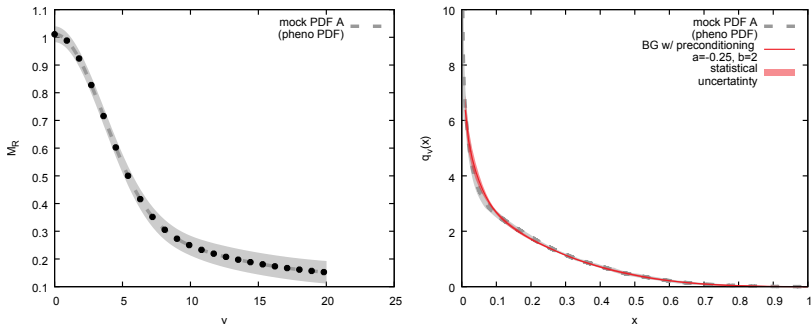
$$\chi[q] = \int_0^1 dx (x - \bar{x})^2 \sum_{j,k} q_j(\bar{x}) K_j(x) K_k(x) q_k(\bar{x}) + \lambda \int_0^1 dx \sum_j K_j(x) q_j(\bar{x}).$$

- But let's see all this in practise ...

Backus-Gilbert reconstruction



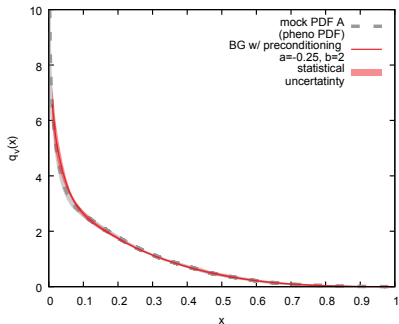
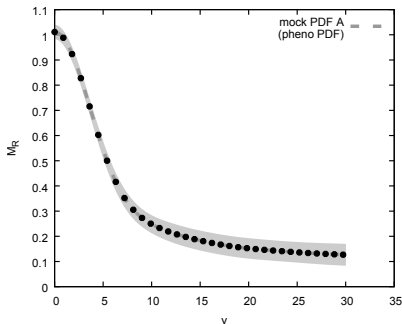
Backus-Gilbert Reconstruction



Left: The NNP31_nlo_as_0118 loffe time PDF data points used in this example, together with the dashed curve from which the data are chosen.

Right: The reconstructed Backus-Gilbert reconstructed PDF (red) together with the original PDF from the NNP31_nlo_as_0118 dataset (blue) with $b = 2$ and $\nu_{max} = 20$.

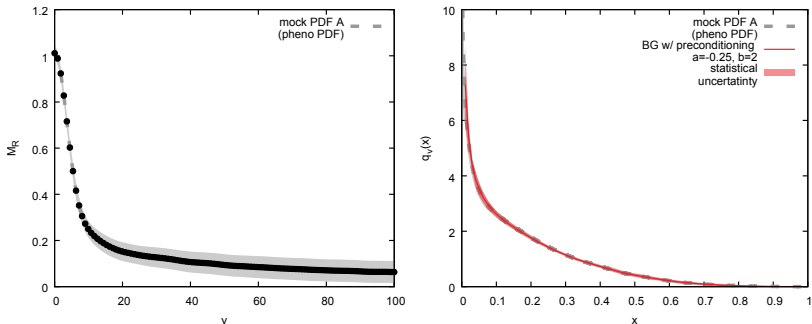
Backus-Gilbert Reconstruction



Left: The NNP31_nlo_as_0118 loffe time PDF data points used in this example, together with the dashed curve from which the data are chosen.

Right: The reconstructed Backus-Gilbert reconstructed PDF (red) together with the original PDF from the NNP31_nlo_as_0118 dataset (blue) with $b = 2$ and $\nu_{max} = 30$.

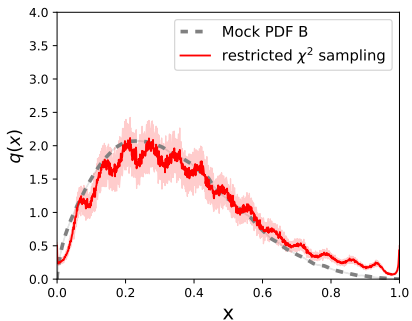
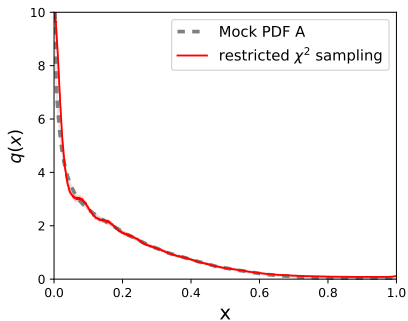
Backus-Gilbert Reconstruction



Left: The NNP31_nlo_as_0118 loffe time PDF data points used in this example, together with the dashed curve from which the data are chosen.

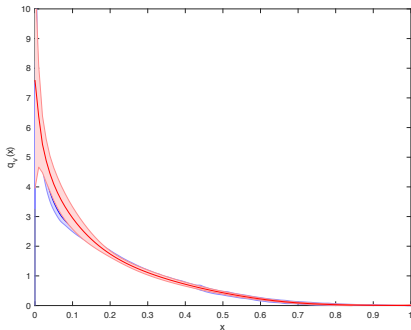
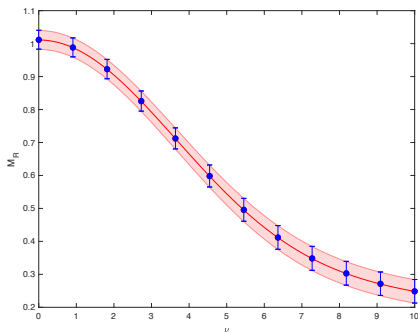
Right: The reconstructed Backus-Gilbert reconstructed PDF (red) together with the original PDF from the NNP31_nlo_as_0118 dataset (blue) with $b = 2$ and $\nu_{max} = 100$.

HMC Reconstruction (Preliminary)



Neural Network Reconstruction

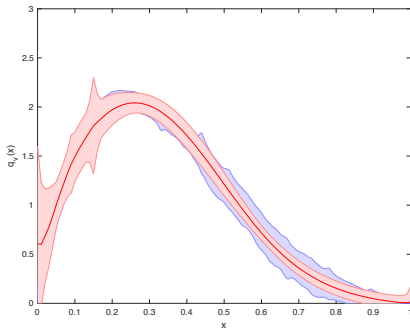
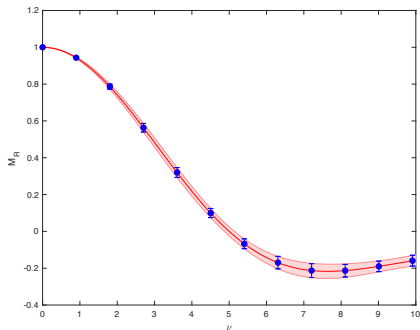
VERY PRELIMINARY RESULTS!!!



Left: Original data points (red) not visible. Red band representing errors on the original data points. Reconstructed data points (blue). **Right:** Original PDF (blue). Reconstructed PDF (red).

Neural Network Reconstruction

VERY PRELIMINARY RESULTS!!!



Left: Original data points (red) not visible. Red band representing errors on the original data points. Reconstructed data points (blue). **Right:** Original PDF (blue). Reconstructed PDF (red).

Conclusions and outlook

- We presented a new approach for obtaining PDFs from lattice QCD calculations
- Using an appropriate ratio of ME we were able to get rid of UV divergences ensuring a well defined continuum limit
- One can scan in loffe time ν which is the Fourier dual to the momentum fraction x by using the hadron momentum
- Large hadron momentum is required to access the large ν -regime or equivalently small- x physics
- To approach the light cone we need to send $z_3^2 \rightarrow 0$ keeping ν fixed
- The pseudo-PDF ratio lead to suppression of scaling violations in z_3^2
- The observed z^2 dependence is compatible with DGLAP evolution

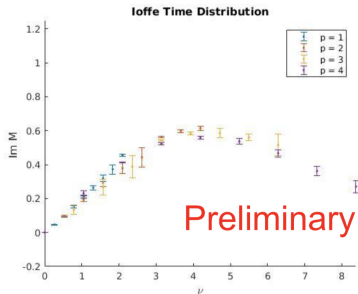
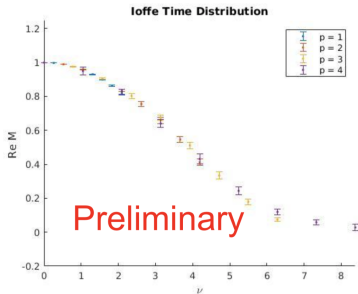
Conclusions and outlook

- Remember, that PDFs are needed as theoretical inputs to all hadron scattering experiments and in some cases are the largest theory uncertainty.
- In the absence of extensive experimental data, first principles calculations of PDFs will significantly improve PDF uncertainties . The interplay between lattice QCD and global fits [H.-W. Lin et al., Prog. Part. Nucl. Phys. 100 \(2018\) 107](#) , where it was demonstrated that the impact of lattice calculations of both the lowest Mellin moments and the x -dependence of PDFs could significantly reduce uncertainties in global PDF fits. For example, lattice determinations of the $\bar{d}(x, Q^2)$ PDF at moderate values of x with uncertainties of 5– 10% could reduce the corresponding PDF uncertainties by up to 30–50%.
- In the search of New Physics we need a precise knowledge of the PDFs from the lattice because the current method of global fits assumes the results of scattering experiments are just convolutions of known parton scattering and of unknown PDFs. If there is New Physics affecting that event it would be absorbed into the PDF.

Conclusions-Outlook

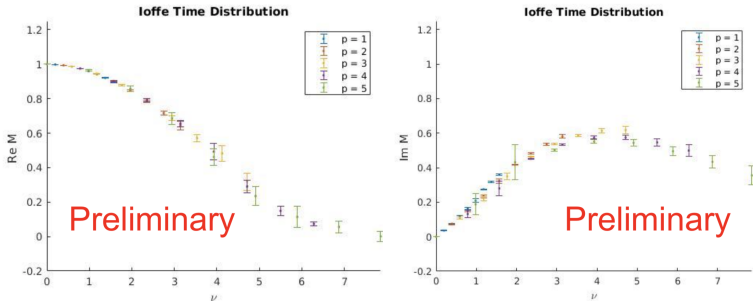
- We studied the problem of PDF reconstructions out of lattice time data: an extremely ill-defined problem due to restricted range and number of ν data.
- We showed how methods of advanced reconstruction that have been successfully applied to different inverse problems in LQCD can also become handy for this task.
- We stressed the necessity of additional info in order to be able to provide a unique answer.
- Soon we will be finalizing our results with $2 + 1$ dynamical flavors of Wilson clover fermions which will include a more detailed study of all involved systematics (discretization effects, finite-volume effects, lighter pions, excited state contamination etc)
- These methods would be key ingredients of future studies.
- **Many thanks for your attention!!!**

Preliminary results with unquenched lattices



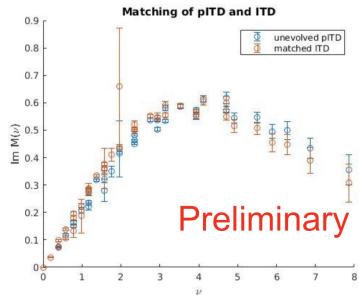
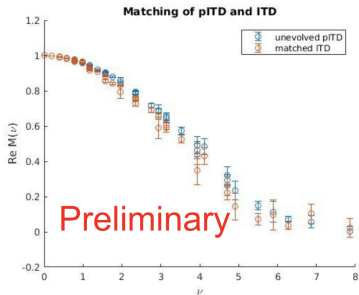
$V = 24^3 \times 64$, with $m_\pi = 440\text{MeV}$ and $a = 0.127\text{fm}$

Preliminary results with unquenched lattices



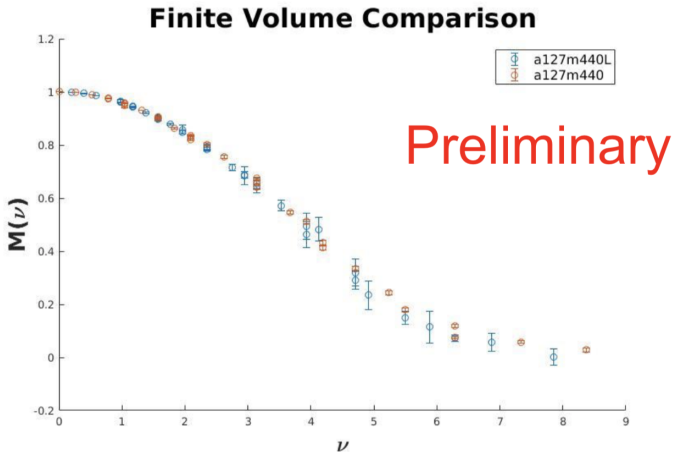
$V = 32^3 \times 64$, with $m_\pi = 440\text{MeV}$ and $a = 0.127\text{fm}$

Unquenched results - matched to \overline{MS}



$V = 32^3 \times 64$, with $m_\pi = 440\text{MeV}$ and $a = 0.127\text{fm}$

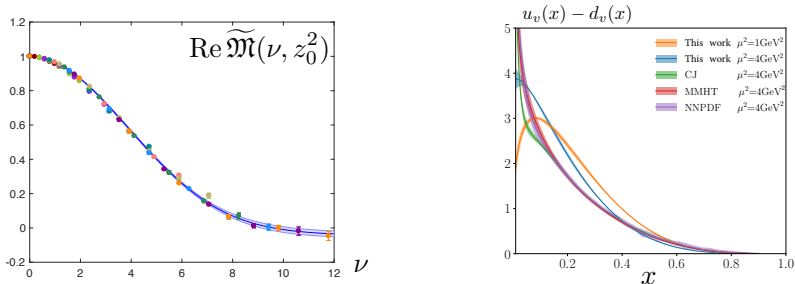
Preliminary results with unquenched lattices



A comparison between two different volumes. Two Current matrix elements can have very large finite volume corrections (Briceño et al Phys.Rev. D98 (2018) 014511, Bali et al.

(2018) 1807.03073)

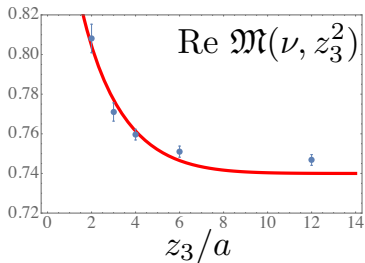
Comparison to global fits



LHS: Data points for $\text{Re } \widetilde{\mathcal{M}}(\nu, z_3^2)$ with $z_3 \leq 10a$ evolved to $z_3 = 2a$. By fitting these evolved points with a cosine FT of $q_v(x) = N(a, b)x^a(1-x)^b$ we obtain $a = 0.36(6)$ and $b = 3.95(22)$ (statistical errors). RHS: Curve for $u_v(x) - d_v(x)$ built from the evolved data shown in the left panel and treated as corresponding to the $\mu^2 = 1 \text{ GeV}^2$ scale; then evolved to the reference point $\mu^2 = 4 \text{ GeV}^2$ of the global fits. 1-loop matching to $\overline{\text{MS}}$ still to be done on our data

A. Radyushkin 1710.08813, Zhang et al 1801.03023, Izubuchi et al 1801.03917

More on evolution



- LO evolution cannot be extended to very low scales.
- It is known that evolution stops below a certain scale (by observing our data we infer that this is the case for $z_3 \geq 6a$.)
- Adopt an evolution that leaves the PDF unchanged for length scales above $z_3 = 6a$ and use the leading perturbative evolution formula to evolve to smaller z_3 scales.

Numerical implementation

Following [C. Bouchard et.al Phys. Rev. D 96, no. 1, 014504 \(2017\)](#) , we compute a regular nucleon two point function

$$C_p(t) = \langle \mathcal{N}_p(t) \overline{\mathcal{N}}_p(0) \rangle ,$$

$$C_p^{\mathcal{O}^0(z)}(t) = \sum_{\tau} \langle \mathcal{N}_p(t) \mathcal{O}^0(z, \tau) \overline{\mathcal{N}}_p(0) \rangle$$

$$\text{with } \mathcal{O}^0(z, t) = \overline{\psi}(0, t) \gamma^0 \tau_3 \hat{E}(0, z; A) \psi(z, t)$$

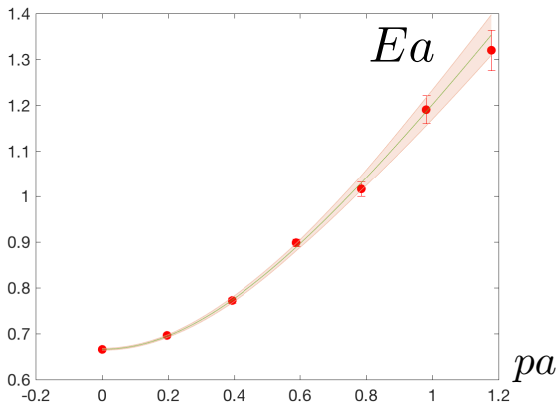
Proton momentum and displacement of the quark fields along the \hat{z} axis

$$\mathcal{M}_{\text{eff}}(z_3 p, z_3^2; t) = \frac{C_p^{\mathcal{O}^0(z)}(t+1)}{C_p(t+1)} - \frac{C_p^{\mathcal{O}^0(z)}(t)}{C_p(t)}$$

Extract the desired ME \mathcal{J} at large Euclidean time separation as

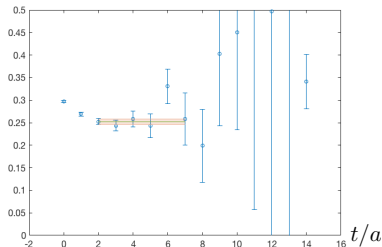
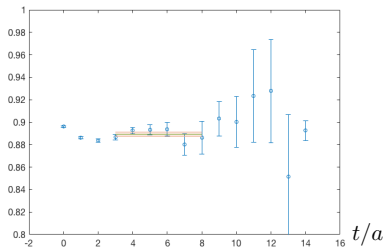
$$\frac{\mathcal{J}(z_3 p, z_3^2)}{2p^0} = \lim_{t \rightarrow \infty} \mathcal{M}_{\text{eff}}(z_3 p, z_3^2; t) , \text{ where } p^0 \text{ is the energy of the nucleon.}$$

Results for the nucleon dispersion relation



Energies and momenta are in lattice units. The solid line is the continuum dispersion relation (not a fit) while the errorband is an indication of the statistical error of the lattice nucleon energies

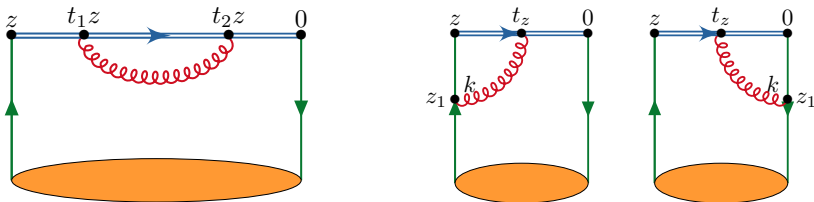
Results



Typical fits used to extract the reduced matrix element (here $p = 2\pi/L \cdot 2$ and $z = 4$ (LHS) and $p = 2\pi/L \cdot 3$ and $z = 8$ (RHS)). The average χ^2 per degree of freedom was $\mathcal{O}(1)$. All fits are performed with the full covariance matrix and the error bars are determined with the jackknife method.

Renormalization

- In a series of articles [Dotsenko Nucl.Phys. B169 \(1980\) 527](#), [Ishikawa et al. Phys. Rev. D 96, 094019 \(2017\)](#), [Chen et al. Nucl.Phys. B915 \(2017\)](#) and [A. V. Radyushkin Phys.Lett. B781 \(2018\) 433-442](#) the one loop renormalizability of $\mathcal{M}^\alpha(z, p, a)$ has been discussed
- by analyzing the pertinent diagrams one can see that there is a linear divergence from the link self-energy contribution and a logarithmic divergence associated to the anomalous dimension $2\gamma_{\text{end}}$ due to two end-points of the link.



Renormalization

- \mathcal{M} has been shown to renormalize multiplicatively as $\mathcal{M}_R(\nu, z^2, \mu) = Z_j^{-1} Z_{\bar{j}}^{-1} e^{-\delta m |z|} \mathcal{M}_B(\nu, z^2, a)$, where $\delta m = C_F \frac{\alpha_s}{2\pi} \frac{\pi}{a}$, is an effective mass counterterm removing power divergences in the Wilson line and $Z_j^{-1}, Z_{\bar{j}}^{-1}$ are renormalization constants (RCs) associated with the endpoints of the Wilson line independent of z, p .
- The entire renormalization is independent of the external momentum
- Forming the ratio, the RCs cancel and thus the reduced Ioffe time distribution has a great potential to reduce systematic effects related to renormalization. The UV divergences generated by the link-related and quark-self-energy diagrams cancel in the ratio.

Numerical implementation

- Renormalization of the ME?
- For $z_3 = 0$ $\mathcal{M}(z_3 p, z_3^2) \rightarrow$ the local iso-vector current, should be = 1 (but ...) lattice artifacts...
- Introduce an RC $Z_p = \frac{1}{\mathcal{J}(z_3 p, z_3^2)|_{z_3=0}}$
- Z_p has to be independent from p . But lattice artifacts or potential fitting systematics ...
- renormalize the ME for each momentum with its own $Z_p \rightarrow$ maximal statistical correlations to reduce statistical errors, and cancellation of lattice artifacts in the ratio

Numerical implementation

- in practise use the double ratio

$$\mathfrak{M}(\nu, z_3^2) = \lim_{t \rightarrow \infty} \frac{\mathcal{M}_{\text{eff}}(z_3 p, z_3^2; t)}{\mathcal{M}_{\text{eff}}(z_3 p, z_3^2; t)|_{z_3=0}} \times \frac{\mathcal{M}_{\text{eff}}(z_3 p, z_3^2; t)|_{p=0, z_3=0}}{\mathcal{M}_{\text{eff}}(z_3 p, z_3^2; t)|_{p=0}},$$

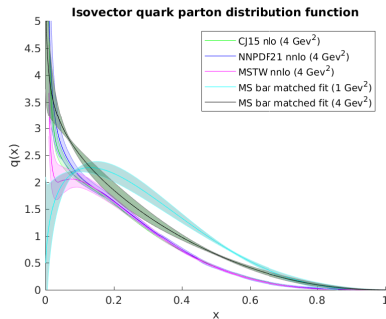
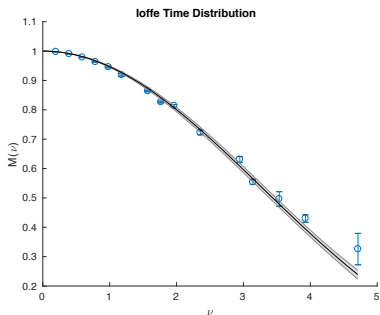
- infinite t limit is obtained with a fit to a constant for a suitable choice of a fitting range.

Matching to \overline{MS}

- In 1801.02427 it was shown by Radyushkin that at 1-loop evolution and matching to \overline{MS} can be done simultaneously.
- This establishes a direct relation between the Ioffe time distribution function (ITDF) and pseudo-ITDF.
- Scales are needed as such that we are in a regime dominated by perturbative effects

$$\begin{aligned} \mathcal{I}(\nu, \mu^2) = & \mathfrak{M}(\nu, z_3^2) + \frac{\alpha_s}{\pi} C_F \int_0^1 dw \mathfrak{M}(w\nu, z_3^2) \\ & \times \left\{ B(w) \ln \left[(1-w) z_3 \mu \frac{e^{\gamma_E + 1/2}}{2} \right] \right. \\ & \left. + [(w+1) \ln(1-w) - (1-w)]_+ \right\} \end{aligned}$$

Comparison to global fits after converting to the \overline{MS} scheme



Bayesian Reconstruction

$$P[q|\mathfrak{M}, I] = \frac{P[\mathfrak{M}|q, I]P[q|I]}{P[\mathfrak{M}|I]}.$$

- The likelihood probability $P[\mathfrak{M}|q, I]$ denotes how probable it is to find the data \mathfrak{M} if q were the correct PDF.
- Finding the most probable q by maximizing the likelihood is nothing but a χ^2 fit to the \mathfrak{M} data, which as we saw from the direct inversion is by itself ill-defined.
- The prior probability $P[q|I]$, which quantifies, how compatible our test function q is with respect to any prior information we have (e.g. appearance of non-analytic behavior of $q(x)$ at the boundaries of the x interval).
- $P[\mathfrak{M}|I]$, the so called evidence is a q independent normalization.

Bayesian Reconstruction

- For sampled data, due to the central limit theorem, the likelihood probability may be written as the quadratic distance functional $P[\mathfrak{M}|q, I] = \exp[-L]$ with $L = \frac{1}{2} \sum_{k,l} (\mathfrak{M}_k - \mathfrak{M}_k^q) C_{kl}^{-1} (\mathfrak{M}_l - \mathfrak{M}_l^q)$.
- \mathfrak{M}_k^q are the loffe-time data arising from inserting the test function q into the cosine Fourier trafo and C_{kl} denotes the covariance matrix of the N_m measurements of simulation data \mathfrak{M}_k^h .
- We then specify an appropriate prior probability $P[q|I] = \exp[\alpha S[I]]$.
- Prior information enters in two ways here. On the one hand we deploy a particular functional form of the regularization functional

$$S_{BR}[q, m] = \sum_n \Delta x_n \left(1 - \frac{q_n}{m_n} + \log\left(\frac{q_n}{m_n}\right) \right)$$

which may be obtained by requiring positive definiteness of the resulting q , smoothness of q .

Bayesian Reconstruction

- For sampled data, due to the central limit theorem, the likelihood probability may be written as the quadratic distance functional $P[\mathfrak{M}|q, I] = \exp[-L]$ with $L = \frac{1}{2} \sum_{k,l} (\mathfrak{M}_k - \mathfrak{M}_k^q) C_{kl}^{-1} (\mathfrak{M}_l - \mathfrak{M}_l^q)$.
- \mathfrak{M}_k^q are the loffe-time data arising from inserting the test function q into the cosine Fourier trafo and C_{kl} denotes the covariance matrix of the N_m measurements of simulation data \mathfrak{M}_k^h .
- We then specify an appropriate prior probability $P[q|I] = \exp[\alpha S[I]]$.
- Prior information enters in two ways here. On the one hand we deploy a particular functional form of the regularization functional

$$S_{BR}[q, m] = \sum_n \Delta x_n \left(1 - \frac{q_n}{m_n} + \log\left(\frac{q_n}{m_n}\right) \right)$$

which may be obtained by requiring positive definiteness of the resulting q , smoothness of q .

Bayesian Reconstruction

- For sampled data, due to the central limit theorem, the likelihood probability may be written as the quadratic distance functional $P[\mathfrak{M}|q, I] = \exp[-L]$ with $L = \frac{1}{2} \sum_{k,l} (\mathfrak{M}_k - \mathfrak{M}_k^q) C_{kl}^{-1} (\mathfrak{M}_l - \mathfrak{M}_l^q)$.
- \mathfrak{M}_k^q are the loffe-time data arising from inserting the test function q into the cosine Fourier trafo and C_{kl} denotes the covariance matrix of the N_m measurements of simulation data \mathfrak{M}_k^h .
- We then specify an appropriate prior probability $P[q|I] = \exp[\alpha S[I]]$.
- Prior information enters in two ways here. On the one hand we deploy a particular functional form of the regularization functional

$$S_{BR}[q, m] = \sum_n \Delta x_n \left(1 - \frac{q_n}{m_n} + \log\left(\frac{q_n}{m_n}\right) \right)$$

which may be obtained by requiring positive definiteness of the resulting q , smoothness of q .

Bayesian Reconstruction

- For sampled data, due to the central limit theorem, the likelihood probability may be written as the quadratic distance functional $P[\mathfrak{M}|q, I] = \exp[-L]$ with $L = \frac{1}{2} \sum_{k,l} (\mathfrak{M}_k - \mathfrak{M}_k^q) C_{kl}^{-1} (\mathfrak{M}_l - \mathfrak{M}_l^q)$.
- \mathfrak{M}_k^q are the loffe-time data arising from inserting the test function q into the cosine Fourier trafo and C_{kl} denotes the covariance matrix of the N_m measurements of simulation data \mathfrak{M}_k^h .
- We then specify an appropriate prior probability $P[q|I] = \exp[\alpha S[I]]$.
- Prior information enters in two ways here. On the one hand we deploy a particular functional form of the regularization functional

$$S_{BR}[q, m] = \sum_n \Delta x_n \left(1 - \frac{q_n}{m_n} + \log\left(\frac{q_n}{m_n}\right) \right)$$

which may be obtained by requiring positive definiteness of the resulting q , smoothness of q .

Bayesian Reconstruction

- The functional S depends on the function m , the default model.
- By construction constitutes its unique extremum.
- In the Bayesian logic m is the correct result for q in the absence of any data.
- We select m by a best fit of the lattice-PDF data and we will vary it to get a handle on systematics.

Bayesian Reconstruction

- The functional S depends on the function m , the default model.
- By construction constitutes its unique extremum.
- In the Bayesian logic m is the correct result for q in the absence of any data.
- We select m by a best fit of the Ioffe-PDF data and we will vary it to get a handle on systematics.

Bayesian Reconstruction

- The functional S depends on the function m , the default model.
- By construction constitutes its unique extremum.
- In the Bayesian logic m is the correct result for q in the absence of any data.
- We select m by a best fit of the lattice-PDF data and we will vary it to get a handle on systematics.

Bayesian Reconstruction

- The functional S depends on the function m , the default model.
- By construction constitutes its unique extremum.
- In the Bayesian logic m is the correct result for q in the absence of any data.
- We select m by a best fit of the Ioffe-PDF data and we will vary it to get a handle on systematics.

Bayesian Reconstruction

- What happens in the case of non-guaranteed positive definiteness?
- We need to change the regulator!
- Often the quadratic regulator is used

$$S_{QDR}[q, m] = \sum_n \Delta x_n (q_n - m_n)^2$$

- It is a comparatively strong regulator and usually imprints the form of the default model significantly onto the end result.
- Trying to keep the influence of the default model to a minimum, we extend the BR prior to non-positive functions.

$$S_{BRg}[q, m] = \sum_n \Delta x_n \left(-\frac{|q_n - m_n|}{h_n} + \log\left(\frac{|q_n - m_n|}{h_n} - 1\right) \right)$$

keeping the advantageous properties of the original BR prior at the price of having to introduce another default model related function h .

Bayesian Reconstruction

- What happens in the case of non-guaranteed positive definiteness?
- We need to change the regulator!
- Often the quadratic regulator is used

$$S_{QDR}[q, m] = \sum_n \Delta x_n (q_n - m_n)^2$$

- It is a comparatively strong regulator and usually imprints the form of the default model significantly onto the end result.
- Trying to keep the influence of the default model to a minimum, we extend the BR prior to non-positive functions.

$$S_{BRg}[q, m] = \sum_n \Delta x_n \left(-\frac{|q_n - m_n|}{h_n} + \log\left(\frac{|q_n - m_n|}{h_n} - 1\right) \right)$$

keeping the advantageous properties of the original BR prior at the price of having to introduce another default model related function h .

Bayesian Reconstruction

- What happens in the case of non-guaranteed positive definiteness?
- We need to change the regulator!
- Often the quadratic regulator is used

$$S_{QDR}[q, m] = \sum_n \Delta x_n (q_n - m_n)^2$$

- It is a comparatively strong regulator and usually imprints the form of the default model significantly onto the end result.
- Trying to keep the influence of the default model to a minimum, we extend the BR prior to non-positive functions.

$$S_{BRg}[q, m] = \sum_n \Delta x_n \left(-\frac{|q_n - m_n|}{h_n} + \log\left(\frac{|q_n - m_n|}{h_n} - 1\right) \right)$$

keeping the advantageous properties of the original BR prior at the price of having to introduce another default model related function h .

Bayesian Reconstruction

- What happens in the case of non-guaranteed positive definiteness?
- We need to change the regulator!
- Often the quadratic regulator is used

$$S_{QDR}[q, m] = \sum_n \Delta x_n (q_n - m_n)^2$$

- It is a comparatively strong regulator and usually imprints the form of the default model significantly onto the end result.
- Trying to keep the influence of the default model to a minimum, we extend the BR prior to non-positive functions.

$$S_{BRg}[q, m] = \sum_n \Delta x_n \left(-\frac{|q_n - m_n|}{h_n} + \log\left(\frac{|q_n - m_n|}{h_n} - 1\right) \right)$$

keeping the advantageous properties of the original BR prior at the price of having to introduce another default model related function h .

Bayesian Reconstruction

- What happens in the case of non-guaranteed positive definiteness?
- We need to change the regulator!
- Often the quadratic regulator is used

$$S_{QDR}[q, m] = \sum_n \Delta x_n (q_n - m_n)^2$$

- It is a comparatively strong regulator and usually imprints the form of the default model significantly onto the end result.
- Trying to keep the influence of the default model to a minimum, we extend the BR prior to non-positive functions.

$$S_{BRg}[q, m] = \sum_n \Delta x_n \left(-\frac{|q_n - m_n|}{h_n} + \log\left(\frac{|q_n - m_n|}{h_n} - 1\right) \right)$$

keeping the advantageous properties of the original BR prior at the price of having to introduce another default model related function h .

Bayesian Reconstruction

- once L , S and m have been provided, the most probable PDF q , given simulation data and prior information is obtained by numerically finding the extremum of the posterior

$$\left. \frac{\delta P[q|\mathfrak{M}, I]}{\delta q} \right|_{q=q_{\text{Bayes}}} = 0.$$

- It has been proven that if the regulator is strictly concave, as is the case for all the regulators discussed above, there only exists a single unique extremum in the space of functions q on a discrete ν interval.
- With positive definiteness imposed on the end result, the space of admissible solutions is significantly reduced. Regulators admitting also q functions with negative contributions have to distinguish between a multitude of oscillatory functions, which if integrated over, resemble a monotonous function to high precision. We will observe the emergence of ringing artefacts for the quadratic and generalized BR prior.

Bayesian Reconstruction

- once L , S and m have been provided, the most probable PDF q , given simulation data and prior information is obtained by numerically finding the extremum of the posterior

$$\left. \frac{\delta P[q|\mathfrak{M}, I]}{\delta q} \right|_{q=q_{\text{Bayes}}} = 0.$$

- It has been proven that if the regulator is strictly concave, as is the case for all the regulators discussed above, there only exists a single unique extremum in the space of functions q on a discrete ν interval.
- With positive definiteness is imposed on the end result, the space of admissible solutions is significantly reduced. Regulators admitting also q functions with negative contributions have to distinguish between a multitude of oscillatory functions, which if integrated over, resemble a monotonous function to high precision. We will observe the emergence of ringing artefacts for the quadratic and generalized BR prior.

Bayesian Reconstruction

- once L , S and m have been provided, the most probable PDF q , given simulation data and prior information is obtained by numerically finding the extremum of the posterior

$$\left. \frac{\delta P[q|\mathfrak{M}, I]}{\delta q} \right|_{q=q_{\text{Bayes}}} = 0.$$

- It has been proven that if the regulator is strictly concave, as is the case for all the regulators discussed above, there only exists a single unique extremum in the space of functions q on a discrete ν interval.
- With positive definiteness imposed on the end result, the space of admissible solutions is significantly reduced. Regulators admitting also q functions with negative contributions have to distinguish between a multitude of oscillatory functions, which if integrated over, resemble a monotonous function to high precision. We will observe the emergence of ringing artefacts for the quadratic and generalized BR prior.

Bayesian Reconstruction

- The functional \mathcal{S} depends on the function m , the default model.
- By construction constitutes its unique extremum.
- In the Bayesian logic m is the correct result for q in the absence of any data.
- We select m by a best fit of the loffe-PDF data and we will vary it to get a handle on systematics.
- In the definition of $P[q|I]$ we introduced a further parameter α , a so called hyperparameter
- Weighs the influence of simulation data and prior information. It has to be taken care of self-consistently.
- In the Maximum Entropy Method α is selected, such that the evidence has an extremum. In the BR method we deploy here, we marginalize the parameter α a priori, i.e. we integrate the posterior w.r.t the hyperparameter, assuming complete ignorance of its values $P[\alpha] = 1$.

Bayesian Reconstruction

- The functional \mathcal{S} depends on the function m , the default model.
- By construction constitutes its unique extremum.
- In the Bayesian logic m is the correct result for q in the absence of any data.
- We select m by a best fit of the lattice-PDF data and we will vary it to get a handle on systematics.
- In the definition of $P[q|I]$ we introduced a further parameter α , a so called hyperparameter
- Weighs the influence of simulation data and prior information. It has to be taken care of self-consistently.
- In the Maximum Entropy Method α is selected, such that the evidence has an extremum. In the BR method we deploy here, we marginalize the parameter α a priori, i.e. we integrate the posterior w.r.t the hyperparameter, assuming complete ignorance of its values $P[\alpha] = 1$.

Bayesian Reconstruction

- The functional S depends on the function m , the default model.
- By construction constitutes its unique extremum.
- In the Bayesian logic m is the correct result for q in the absence of any data.
- We select m by a best fit of the lattice-PDF data and we will vary it to get a handle on systematics.
- In the definition of $P[q|I]$ we introduced a further parameter α , a so called hyperparameter
- Weighs the influence of simulation data and prior information. It has to be taken care of self-consistently.
- In the Maximum Entropy Method α is selected, such that the evidence has an extremum. In the BR method we deploy here, we marginalize the parameter α a priori, i.e. we integrate the posterior w.r.t the hyperparameter, assuming complete ignorance of its values $P[\alpha] = 1$.

Bayesian Reconstruction

- The functional S depends on the function m , the default model.
- By construction constitutes its unique extremum.
- In the Bayesian logic m is the correct result for q in the absence of any data.
- We select m by a best fit of the Ioffe-PDF data and we will vary it to get a handle on systematics.
- In the definition of $P[q|I]$ we introduced a further parameter α , a so called hyperparameter
- Weighs the influence of simulation data and prior information. It has to be taken care of self-consistently.
- In the Maximum Entropy Method α is selected, such that the evidence has an extremum. In the BR method we deploy here, we marginalize the parameter α a priori, i.e. we integrate the posterior w.r.t the hyperparameter, assuming complete ignorance of its values $P[\alpha] = 1$.

Bayesian Reconstruction

- The functional S depends on the function m , the default model.
- By construction constitutes its unique extremum.
- In the Bayesian logic m is the correct result for q in the absence of any data.
- We select m by a best fit of the Ioffe-PDF data and we will vary it to get a handle on systematics.
- In the definition of $P[q|I]$ we introduced a further parameter α , a so called hyperparameter
 - Weighs the influence of simulation data and prior information. It has to be taken care of self-consistently.
 - In the Maximum Entropy Method α is selected, such that the evidence has an extremum. In the BR method we deploy here, we marginalize the parameter α a priori, i.e. we integrate the posterior w.r.t the hyperparameter, assuming complete ignorance of its values $P[\alpha] = 1$.

Bayesian Reconstruction

- The functional S depends on the function m , the default model.
- By construction constitutes its unique extremum.
- In the Bayesian logic m is the correct result for q in the absence of any data.
- We select m by a best fit of the Ioffe-PDF data and we will vary it to get a handle on systematics.
- In the definition of $P[q|I]$ we introduced a further parameter α , a so called hyperparameter
- Weighs the influence of simulation data and prior information. It has to be taken care of self-consistently.
- In the Maximum Entropy Method α is selected, such that the evidence has an extremum. In the BR method we deploy here, we marginalize the parameter α a priori, i.e. we integrate the posterior w.r.t the hyperparameter, assuming complete ignorance of its values $P[\alpha] = 1$.

Bayesian Reconstruction

- The functional S depends on the function m , the default model.
- By construction constitutes its unique extremum.
- In the Bayesian logic m is the correct result for q in the absence of any data.
- We select m by a best fit of the Ioffe-PDF data and we will vary it to get a handle on systematics.
- In the definition of $P[q|I]$ we introduced a further parameter α , a so called hyperparameter
- Weighs the influence of simulation data and prior information. It has to be taken care of self-consistently.
- In the Maximum Entropy Method α is selected, such that the evidence has an extremum. In the BR method we deploy here, we marginalize the parameter α a priori, i.e. we integrate the posterior w.r.t the hyperparameter, assuming complete ignorance of its values $P[\alpha] = 1$.

Bayesian Reconstruction

$$P[q|\mathfrak{M}, I] = \frac{P[\mathfrak{M}|q, I]P[q|I]}{P[\mathfrak{M}|I]}.$$

- The likelihood probability $P[\mathfrak{M}|q, I]$ denotes how probable it is to find the data \mathfrak{M} if q were the correct PDF.
- Finding the most probable q by maximizing the likelihood is nothing but a χ^2 fit to the \mathfrak{M} data, which as we saw from the direct inversion is by itself ill-defined.
- The prior probability $P[q|I]$, which quantifies, how compatible our test function q is with respect to any prior information we have (e.g. appearance of non-analytic behavior of $q(x)$ at the boundaries of the x interval).
- $P[\mathfrak{M}|I]$, the so called evidence is a q independent normalization.

Bayesian Reconstruction

- For sampled data, due to the central limit theorem, the likelihood probability may be written as the quadratic distance functional $P[\mathfrak{M}|q, I] = \exp[-L]$ with $L = \frac{1}{2} \sum_{k,l} (\mathfrak{M}_k - \mathfrak{M}_k^q) C_{kl}^{-1} (\mathfrak{M}_l - \mathfrak{M}_l^q)$.
- \mathfrak{M}_k^q are the loffe-time data arising from inserting the test function q into the cosine Fourier trafo and C_{kl} denotes the covariance matrix of the N_m measurements of simulation data \mathfrak{M}_k^h .
- We then specify an appropriate prior probability $P[q|I] = \exp[\alpha S[I]]$.
- Prior information enters in two ways here. On the one hand we deploy a particular functional form of the regularization functional

$$S_{BR}[q, m] = \sum_n \Delta x_n \left(1 - \frac{q_n}{m_n} + \log\left(\frac{q_n}{m_n}\right) \right)$$

which may be obtained by requiring positive definiteness of the resulting q , smoothness of q .

Bayesian Reconstruction

- For sampled data, due to the central limit theorem, the likelihood probability may be written as the quadratic distance functional $P[\mathfrak{M}|q, I] = \exp[-L]$ with $L = \frac{1}{2} \sum_{k,l} (\mathfrak{M}_k - \mathfrak{M}_k^q) C_{kl}^{-1} (\mathfrak{M}_l - \mathfrak{M}_l^q)$.
- \mathfrak{M}_k^q are the loffe-time data arising from inserting the test function q into the cosine Fourier trafo and C_{kl} denotes the covariance matrix of the N_m measurements of simulation data \mathfrak{M}_k^h .
- We then specify an appropriate prior probability $P[q|I] = \exp[\alpha S[I]]$.
- Prior information enters in two ways here. On the one hand we deploy a particular functional form of the regularization functional

$$S_{BR}[q, m] = \sum_n \Delta x_n \left(1 - \frac{q_n}{m_n} + \log\left(\frac{q_n}{m_n}\right) \right)$$

which may be obtained by requiring positive definiteness of the resulting q , smoothness of q .

Bayesian Reconstruction

- For sampled data, due to the central limit theorem, the likelihood probability may be written as the quadratic distance functional $P[\mathfrak{M}|q, I] = \exp[-L]$ with $L = \frac{1}{2} \sum_{k,l} (\mathfrak{M}_k - \mathfrak{M}_k^q) C_{kl}^{-1} (\mathfrak{M}_l - \mathfrak{M}_l^q)$.
- \mathfrak{M}_k^q are the loffe-time data arising from inserting the test function q into the cosine Fourier trafo and C_{kl} denotes the covariance matrix of the N_m measurements of simulation data \mathfrak{M}_k^h .
- We then specify an appropriate prior probability $P[q|I] = \exp[\alpha S[I]]$.
- Prior information enters in two ways here. On the one hand we deploy a particular functional form of the regularization functional

$$S_{BR}[q, m] = \sum_n \Delta x_n \left(1 - \frac{q_n}{m_n} + \log\left(\frac{q_n}{m_n}\right) \right)$$

which may be obtained by requiring positive definiteness of the resulting q , smoothness of q .

Bayesian Reconstruction

- For sampled data, due to the central limit theorem, the likelihood probability may be written as the quadratic distance functional $P[\mathfrak{M}|q, I] = \exp[-L]$ with $L = \frac{1}{2} \sum_{k,l} (\mathfrak{M}_k - \mathfrak{M}_k^q) C_{kl}^{-1} (\mathfrak{M}_l - \mathfrak{M}_l^q)$.
- \mathfrak{M}_k^q are the loffe-time data arising from inserting the test function q into the cosine Fourier trafo and C_{kl} denotes the covariance matrix of the N_m measurements of simulation data \mathfrak{M}_k^h .
- We then specify an appropriate prior probability $P[q|I] = \exp[\alpha S[I]]$.
- Prior information enters in two ways here. On the one hand we deploy a particular functional form of the regularization functional

$$S_{BR}[q, m] = \sum_n \Delta x_n \left(1 - \frac{q_n}{m_n} + \log\left(\frac{q_n}{m_n}\right) \right)$$

which may be obtained by requiring positive definiteness of the resulting q , smoothness of q .

Bayesian Reconstruction

- The functional S depends on the function m , the default model.
- By construction constitutes its unique extremum.
- In the Bayesian logic m is the correct result for q in the absence of any data.
- We select m by a best fit of the lattice-PDF data and we will vary it to get a handle on systematics.

Bayesian Reconstruction

- The functional S depends on the function m , the default model.
- By construction constitutes its unique extremum.
- In the Bayesian logic m is the correct result for q in the absence of any data.
- We select m by a best fit of the Ioffe-PDF data and we will vary it to get a handle on systematics.

Bayesian Reconstruction

- The functional S depends on the function m , the default model.
- By construction constitutes its unique extremum.
- In the Bayesian logic m is the correct result for q in the absence of any data.
- We select m by a best fit of the lattice-PDF data and we will vary it to get a handle on systematics.

Bayesian Reconstruction

- The functional S depends on the function m , the default model.
- By construction constitutes its unique extremum.
- In the Bayesian logic m is the correct result for q in the absence of any data.
- We select m by a best fit of the Ioffe-PDF data and we will vary it to get a handle on systematics.

Bayesian Reconstruction

- What happens in the case of non-guaranteed positive definiteness?
- We need to change the regulator!
- Often the quadratic regulator is used

$$S_{QDR}[q, m] = \sum_n \Delta x_n (q_n - m_n)^2$$

- It is a comparatively strong regulator and usually imprints the form of the default model significantly onto the end result.
- Trying to keep the influence of the default model to a minimum, we extend the BR prior to non-positive functions.

$$S_{BRg}[q, m] = \sum_n \Delta x_n \left(-\frac{|q_n - m_n|}{h_n} + \log\left(\frac{|q_n - m_n|}{h_n} - 1\right) \right)$$

keeping the advantageous properties of the original BR prior at the price of having to introduce another default model related function h .

Bayesian Reconstruction

- What happens in the case of non-guaranteed positive definiteness?
- We need to change the regulator!
- Often the quadratic regulator is used

$$S_{QDR}[q, m] = \sum_n \Delta x_n (q_n - m_n)^2$$

- It is a comparatively strong regulator and usually imprints the form of the default model significantly onto the end result.
- Trying to keep the influence of the default model to a minimum, we extend the BR prior to non-positive functions.

$$S_{BRg}[q, m] = \sum_n \Delta x_n \left(-\frac{|q_n - m_n|}{h_n} + \log\left(\frac{|q_n - m_n|}{h_n} - 1\right) \right)$$

keeping the advantageous properties of the original BR prior at the price of having to introduce another default model related function h .

Bayesian Reconstruction

- What happens in the case of non-guaranteed positive definiteness?
- We need to change the regulator!
- Often the quadratic regulator is used

$$S_{QDR}[q, m] = \sum_n \Delta x_n (q_n - m_n)^2$$

- It is a comparatively strong regulator and usually imprints the form of the default model significantly onto the end result.
- Trying to keep the influence of the default model to a minimum, we extend the BR prior to non-positive functions.

$$S_{BRg}[q, m] = \sum_n \Delta x_n \left(-\frac{|q_n - m_n|}{h_n} + \log\left(\frac{|q_n - m_n|}{h_n} - 1\right) \right)$$

keeping the advantageous properties of the original BR prior at the price of having to introduce another default model related function h .

Bayesian Reconstruction

- What happens in the case of non-guaranteed positive definiteness?
- We need to change the regulator!
- Often the quadratic regulator is used

$$S_{QDR}[q, m] = \sum_n \Delta x_n (q_n - m_n)^2$$

- It is a comparatively strong regulator and usually imprints the form of the default model significantly onto the end result.
- Trying to keep the influence of the default model to a minimum, we extend the BR prior to non-positive functions.

$$S_{BRg}[q, m] = \sum_n \Delta x_n \left(-\frac{|q_n - m_n|}{h_n} + \log\left(\frac{|q_n - m_n|}{h_n} - 1\right) \right)$$

keeping the advantageous properties of the original BR prior at the price of having to introduce another default model related function h .

Bayesian Reconstruction

- What happens in the case of non-guaranteed positive definiteness?
- We need to change the regulator!
- Often the quadratic regulator is used

$$S_{QDR}[q, m] = \sum_n \Delta x_n (q_n - m_n)^2$$

- It is a comparatively strong regulator and usually imprints the form of the default model significantly onto the end result.
- Trying to keep the influence of the default model to a minimum, we extend the BR prior to non-positive functions.

$$S_{BRg}[q, m] = \sum_n \Delta x_n \left(-\frac{|q_n - m_n|}{h_n} + \log\left(\frac{|q_n - m_n|}{h_n} - 1\right) \right)$$

keeping the advantageous properties of the original BR prior at the price of having to introduce another default model related function h .

Bayesian Reconstruction

- once L , S and m have been provided, the most probable PDF q , given simulation data and prior information is obtained by numerically finding the extremum of the posterior

$$\left. \frac{\delta P[q|\mathfrak{M}, I]}{\delta q} \right|_{q=q_{\text{Bayes}}} = 0.$$

- It has been proven that if the regulator is strictly concave, as is the case for all the regulators discussed above, there only exists a single unique extremum in the space of functions q on a discrete ν interval.
- With positive definiteness imposed on the end result, the space of admissible solutions is significantly reduced. Regulators admitting also q functions with negative contributions have to distinguish between a multitude of oscillatory functions, which if integrated over, resemble a monotonous function to high precision. We will observe the emergence of ringing artefacts for the quadratic and generalized BR prior.

Bayesian Reconstruction

- once L , S and m have been provided, the most probable PDF q , given simulation data and prior information is obtained by numerically finding the extremum of the posterior

$$\left. \frac{\delta P[q|\mathfrak{M}, I]}{\delta q} \right|_{q=q_{\text{Bayes}}} = 0.$$

- It has been proven that if the regulator is strictly concave, as is the case for all the regulators discussed above, there only exists a single unique extremum in the space of functions q on a discrete ν interval.
- With positive definiteness is imposed on the end result, the space of admissible solutions is significantly reduced. Regulators admitting also q functions with negative contributions have to distinguish between a multitude of oscillatory functions, which if integrated over, resemble a monotonous function to high precision. We will observe the emergence of ringing artefacts for the quadratic and generalized BR prior.

Bayesian Reconstruction

- once L , S and m have been provided, the most probable PDF q , given simulation data and prior information is obtained by numerically finding the extremum of the posterior

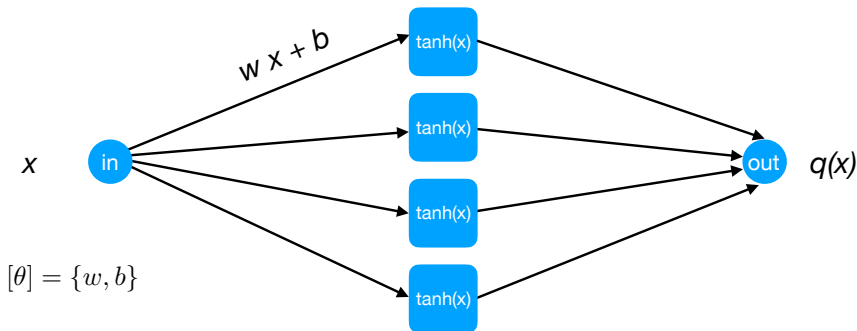
$$\left. \frac{\delta P[q|\mathfrak{M}, I]}{\delta q} \right|_{q=q_{\text{Bayes}}} = 0.$$

- It has been proven that if the regulator is strictly concave, as is the case for all the regulators discussed above, there only exists a single unique extremum in the space of functions q on a discrete ν interval.
- With positive definiteness imposed on the end result, the space of admissible solutions is significantly reduced. Regulators admitting also q functions with negative contributions have to distinguish between a multitude of oscillatory functions, which if integrated over, resemble a monotonous function to high precision. We will observe the emergence of ringing artefacts for the quadratic and generalized BR prior.

Neural Network Reconstruction

- The ensemble average of data is obtained in two steps
 - ▶ Starting from random $[w, b]$, minimize χ^2 to find $[w, b]$.
 - ▶ Repeat 10 times to find 10 different Neural Nets (replicas).
- For each Neural Net, the minimizer is re-run for each jackknife sample to obtain a jackknife estimate $q(x)$ for each replica.
- The central value of $q(x)$ is estimated as the average over jackknife samples and replicas.
- The error is estimated by combining the fluctuations over the jackknife sample and replicas.

Neural Network Reconstruction



$$\chi^2 = \sum_k \left(M(\nu_k) - \int_0^1 dx q_{[\theta]}(x) \cos(\nu_k x) \right)^2 \left(M(\nu_k) - \int_0^1 dx q_{[\theta]}(x) \cos(\nu_k x) \right)$$

$$\min_{[\theta]} [\chi^2] \rightarrow [w, b]$$